



# Search for a third-generation leptoquark coupled to a $\tau$ lepton and a b quark through single, pair, and nonresonant production in proton-proton collisions at $\sqrt{s} = 13$ TeV

The CMS Collaboration\*

## Abstract

A search is presented for a third-generation leptoquark (LQ) coupled exclusively to a  $\tau$  lepton and a b quark. The search is based on proton-proton collision data at a center-of-mass energy of 13 TeV recorded with the CMS detector, corresponding to an integrated luminosity of  $138 \text{ fb}^{-1}$ . Events with  $\tau$  leptons and a varying number of jets originating from b quarks are considered, targeting the single and pair production of LQs, as well as nonresonant  $t$ -channel LQ exchange. An excess is observed in the data with respect to the background expectation in the combined analysis of all search regions. For a benchmark LQ mass of 2 TeV and an LQ-b- $\tau$  coupling strength of 2.5, the excess reaches a local significance of up to 2.8 standard deviations. Upper limits at the 95% confidence level are placed on the LQ production cross section in the LQ mass range 0.5–2.3 TeV, and up to 3 TeV for  $t$ -channel LQ exchange. Leptoquarks are excluded below masses of 1.22–1.88 TeV for different LQ models and varying coupling strengths up to 2.5. The study of nonresonant  $\tau\tau$  production through  $t$ -channel LQ exchange allows lower limits on the LQ mass of up to 2.3 TeV to be obtained.

*Published in the Journal of High Energy Physics as doi:10.1007/JHEP05(2024)311.*



## 1 Introduction

The standard model (SM) of particle physics is remarkably successful in describing matter and its fundamental interactions. In 2012, the discovery of a major missing piece, the Higgs boson, was announced by the ATLAS and CMS experiments [1–3] at the CERN LHC. Despite the many successes of the SM, there are both theoretical and experimental reasons why it is not considered to be the final and most fundamental theory of nature. Measurements of the  $B \rightarrow D\tau\nu$  and  $B \rightarrow D^*\tau\nu$  decay rates reported by the BaBar [4, 5], Belle [6–11], and LHCb [12–16] Collaborations collectively deviate from the SM predictions by about three standard deviations [17]. Leptoquark (LQ) models have received considerable interest in the interpretation of these deviations. Leptoquarks are hypothetical color-triplet scalar or vector bosons, which carry both baryon and lepton quantum numbers, and have fractional electric charge. They are predicted by many theories beyond the SM, such as grand unification [18–25] and models invoking technicolor [26–28] or compositeness [29–31]. An LQ that couples most strongly to third-generation fermions could offer coherent explanations [32–63] for the  $B \rightarrow D\tau\nu$ ,  $B \rightarrow D^*\tau\nu$ , and other B physics anomalies reported by LHCb [64–69] and Belle [70].

The production cross sections in proton-proton (pp) collisions and decay widths of LQs are determined by: the LQ mass  $m_{LQ}$ , its branching fraction  $\beta$  to a charged lepton and a quark, the coupling strength  $\lambda$  of the LQ-lepton-quark vertex, and the coupling parameter  $\kappa$  in the case of vector LQs [71–73]. The LQ can be produced in pairs via gluon fusion or quark-antiquark annihilation, or singly via quark-gluon fusion. However, for large values of the coupling strength  $\lambda$ , the nonresonant production of two leptons via LQ exchange in the  $t$  channel dominates the total cross section [74, 75]. Pair production of LQs is approximately independent of  $\lambda$ , while single production and nonresonant production are not.

Currently, the most stringent limits on the production of an LQ decaying to a  $\tau$  lepton and a b quark come from analyses by the ATLAS Collaboration [76, 77]. Leptoquarks with masses below 1.49–1.96 TeV were excluded in a search for scalar or vector LQ pair production [76], while coupling-dependent limits have been placed in a search for single and nonresonant LQ production [77], excluding scalar (vector) LQ masses of up to 1.53 (2.05) TeV at couplings of  $\lambda = 2.5$ . A search for single production of LQs with the same decay mode was performed by the CMS Collaboration, excluding scalar LQs below masses of 1.05 TeV for  $\lambda = 2.5$  [78]. Other searches for LQs decaying to a t quark and a  $\tau$  lepton or neutrino exploiting the LHC 2016–2018 (2015–2018) data set have been performed by CMS [79, 80] (ATLAS [81, 82]).

This paper presents a search that targets the single and pair production of scalar and vector LQs that decay exclusively to a  $\tau$  lepton and a b quark, and a search for the nonresonant production of a  $\tau$  lepton pair. Example Feynman diagrams of the signal processes at leading order (LO) are shown in Fig. 1. Single and pair production have a resonant final state that includes two  $\tau$  leptons and at least one heavy-flavored jet. Nonresonant production will also have a final state with two  $\tau$  leptons, and potentially additional jets originating from gluon splitting or initial-state radiation.

The search is based on a data sample of pp collisions at a center-of-mass energy of 13 TeV recorded by the CMS experiment in 2016–2018, corresponding to an integrated luminosity of  $138 \text{ fb}^{-1}$ . It exploits several decay channels of the  $\tau$  lepton pair: fully hadronic ( $\tau_h\tau_h$ ), semileptonic ( $e\tau_h, \mu\tau_h$ ), and fully leptonic channels ( $e\mu, \mu\mu$ ). Throughout this paper, electrons and muons are collectively referred to as leptons ( $\ell$ ). Owing to the large branching fraction of the  $\tau_h$  decay, the semileptonic and fully hadronic channels are the most sensitive to an LQ signal, while events with two leptons are primarily used to constrain the SM backgrounds. Candidate events are further categorized according to whether or not at least one high- $p_T$  jet is present

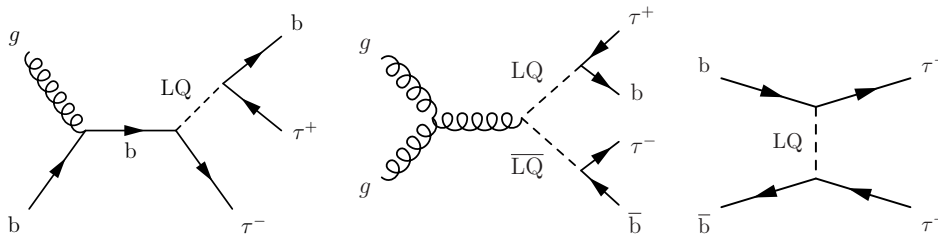


Figure 1: Example Feynman diagrams of signal processes at leading order: single (left) and pair (center) LQ production, as well as nonresonant production of two  $\tau$  leptons via  $t$ -channel LQ exchange (right).

(targeting resonant LQ production) or absent (targeting nonresonant  $\tau\tau$  production). If high- $p_T$  jets are present, two subcategories are defined according to whether or not at least one is identified as being initiated by a  $b$  quark. The LQ signal is extracted from a simultaneous fit to the observed distribution of the scalar sum of transverse momenta in the categories with a high- $p_T$  jet, and the distribution of an angular distribution in the category without a high- $p_T$  jet.

This paper is organized as follows: a brief description of the CMS detector is given in Section 2. The simulated samples used in this analysis are discussed in Section 3, followed by an overview of the event and object reconstruction in Section 4. In Section 5, the event selection and the observables for signal extraction are described, after which the background estimation is described in Section 6. The systematic uncertainties are discussed in Section 7. The results and their statistical interpretation are presented in Section 8. The paper closes with a summary in Section 9.

Tabulated results are provided in the HEPData record for this analysis [83].

## 2 The CMS detector

The central feature of the CMS apparatus is a superconducting solenoid of 6 m internal diameter, providing a magnetic field of 3.8 T. Within the solenoid volume are a silicon pixel and strip tracker, a lead tungstate crystal electromagnetic calorimeter (ECAL), and a brass and scintillator hadron calorimeter (HCAL), each composed of a barrel and two endcap sections. Forward calorimeters extend the pseudorapidity ( $\eta$ ) coverage provided by the barrel and endcap detectors. Muons are measured in gas-ionization detectors embedded in the steel flux-return yoke outside the solenoid. A more detailed description of the CMS detector, together with a definition of the coordinate system used and the relevant kinematic variables, can be found in Ref. [84].

Events of interest are selected using a two-tiered trigger system [85]. The first level, composed of custom hardware processors, uses information from the calorimeters and muon detectors to select events at a rate of around 100 kHz within a time interval of about  $4 \mu\text{s}$  [86]. The second level, known as the high-level trigger, consists of a farm of processors running a version of the full event reconstruction software optimized for fast processing, and reduces the event rate to about 1 kHz before data storage [85].

During the 2016 and 2017 data taking, a gradual shift in the timing of the inputs of the ECAL first-level trigger in the region at  $|\eta| > 2.0$  caused a specific trigger inefficiency. For events containing an electron (a jet) with transverse momentum  $p_T$  larger than  $\approx 50 \text{ GeV}$  ( $\approx 100 \text{ GeV}$ ), in the region  $2.5 < |\eta| < 3.0$  the efficiency loss is  $\approx 10\text{--}20\%$ , depending on  $p_T$ ,  $\eta$ , and time.

Correction factors were computed from data and applied to the kinematic acceptance evaluated by simulation.

### 3 Simulated samples

Samples of simulated events are used to devise selection criteria, and estimate and validate background predictions. The main sources of background are the pair production of  $t$  quarks ( $t\bar{t}$ ), single  $t$  quark production, Drell–Yan (DY) and  $W$  boson production in association with jets, respectively denoted as “DY + jets” and “W + jets”, diboson ( $WW$ ,  $WZ$ ,  $ZZ$ ) production, and quantum chromodynamics (QCD) production of multijet events. The backgrounds are simulated with the Monte Carlo technique, except for the QCD multijet background in the  $\mu\mu$  and  $e\mu$  channels, and the background due to jets misidentified as  $\tau_h$  in the  $\mu\tau_h$ ,  $e\tau_h$ , and  $\tau\tau$  channel. The W + jets and DY + jets processes are generated using the MADGRAPH5\_aMC@NLO [87] generator (versions 2.2.2 and 2.3.3) at LO precision with up to four additional partons simulated at the matrix element level, which are merged and matched to the parton shower with the MLM scheme [88]. Diboson production is generated at LO with PYTHIA [89] in version 8.212 (8.230) for the 2016 (2017 and 2018) sample, except for the gluon-initiated process, which is simulated with the MCFM (version 7.0) generator [90–92]. The  $t\bar{t}$  and single  $t$  quark production are generated by POWHEG [93–95] (versions 2.0 and 1.0) at next-to-LO (NLO) precision in perturbative QCD [96–99].

Minor background processes, denoted in figures and tables as “other”, include electroweak production of  $W$  or  $Z$  bosons in association with jets, the associated production of a  $W$  or  $Z$  boson, a photon, and additional jets ( $V\gamma$  + jets), as well as the production of three massive gauge bosons (triboson production). All minor backgrounds are simulated using different versions of MADGRAPH5\_aMC@NLO depending on the process and data-taking period. The production of a  $Z$  boson and a photon, as well as that of three massive gauge bosons, is simulated at NLO, while all other minor backgrounds are generated at LO.

The DY + jets, W + jets,  $t\bar{t}$ , and single  $t$  processes are normalized using cross sections computed at next-to-NLO (NNLO) in perturbative QCD [100–102]. All other background processes are normalized according to their respective cross sections computed at the same order as that of the matrix element calculations.

A simplified  $\tilde{R}_2$  model [40] is used to generate the signal samples with a scalar LQ. In the case of the vector LQ, a  $U_1$  model [73] is used, in which the LQ couples only to left-handed fermions of the third generation, with a corresponding Lagrangian density  $\mathcal{L} \supset \lambda(\bar{b}_L\gamma^\mu\tau_L U_\mu + \bar{\tau}_L\gamma^\mu\nu_{\tau L} U_\mu) + \text{h.c.}$ . The coupling of LQs to quarks and charged leptons relative to the coupling to quarks and neutrinos is expressed by a dimensionless parameter  $\beta$ . For all signal samples we consider exclusive LQ couplings to  $b$  quarks and  $\tau$  leptons, corresponding to  $\beta = 1$ . The signal samples are generated at LO precision using the MADGRAPH5\_aMC@NLO 2.6.1 [103] event generator with the five-flavor scheme. Since the kinematic properties of the final state are expected to be independent of  $\lambda$  for the LQ signals of  $t$ -channel exchange, pair production, and single production with approximately  $\lambda < 1.5$ , and the LQ decay width is smaller than the experimental resolution, samples generated with  $\lambda = 1$  are used for those cases. Additional samples of single LQ production are generated for values of  $\lambda$  between 1.5–2.5 to take into account the increased width and changes to kinematic properties of the final state. The single and pair production of vector LQs depends on an additional parameter  $\kappa$ , which affects the interaction of the LQ with the SM gauge fields. Values of  $\kappa = 1$  and 0 are considered in this analysis, corresponding to the Yang–Mills and minimal coupling scenarios, respectively. The

nonresonant production of two  $\tau$  leptons via  $t$ -channel LQ exchange is generated assuming no interference with the SM DY process, as the corresponding reduction of the signal yield in sensitive regions of the analysis would be less than 5% for  $\lambda > 1$  [75] and is therefore considered to be negligible. The cross sections of all signal processes are computed at LO with the models discussed above, except for the production of a scalar LQ pair, which is computed at NLO [104–106].

The event generators are interfaced with PYTHIA 8.212 for 2016 and 8.230 for 2017 and 2018 samples to model the parton showering and fragmentation, as well as the decay of the  $\tau$  leptons. The PYTHIA parameters affecting the description of the underlying event are set to the CUETP8M1 (CP5) tune for all 2016 (2017–2018) samples [107, 108], except for the 2016  $t\bar{t}$  sample, for which CUETP8M2T4 [109] is used. For the simulation of the SM background processes, the NNPDF3.0 PDFs [110] with the order matching that of the matrix element calculations are used with all generators for 2016, while NNPDF3.1 [111] NNLO PDFs are used for 2017 and 2018 running conditions. For the simulation of the LQ signal, NNPDF3.1 PDFs at LO are used for all years. Generated events are processed through a simulation of the CMS detector based on GEANT4 [112], and are reconstructed with the same algorithms as used for data. The simulated samples include additional pp interactions per bunch crossing, referred to as “pileup”. The effect of pileup is taken into account by generating minimum-bias collision events with PYTHIA. The simulated events are weighted such that the distribution of the number of pileup interactions matches that in data.

## 4 Event and object reconstruction

A particle-flow algorithm [113] aims to reconstruct and identify each individual particle in an event, with an optimized combination of information from the various elements of the CMS detector. Photons are identified as ECAL energy clusters not linked to the extrapolation of any charged particle trajectory to the ECAL. Electrons are identified as a primary charged particle track and potentially many ECAL energy clusters, corresponding to this track extrapolation to the ECAL and to possible bremsstrahlung photons emitted along the way through the tracker material. Muons are identified as tracks in the central tracker consistent with either a track or several hits in the muon system, and associated with calorimeter deposits compatible with the muon hypothesis. Charged hadrons are identified as charged particle tracks neither identified as electrons, nor as muons. Finally, neutral hadrons are identified as HCAL energy clusters not linked to any charged hadron trajectory, or as a combined ECAL and HCAL energy excess with respect to the expected charged hadron energy deposit.

The energy of photons is obtained from the ECAL measurement. The energy of electrons is determined from a combination of the track momentum at the main interaction vertex, the corresponding ECAL cluster energy, and the energy sum of all bremsstrahlung photons attached to the track. The energy of muons is obtained from the corresponding track momentum. The energy of charged hadrons is determined from a combination of the track momentum and the corresponding ECAL and HCAL energies, corrected for the response function of the calorimeters to hadronic showers. Finally, the energy of neutral hadrons is obtained from the corresponding corrected ECAL and HCAL energies.

The primary pp interaction vertex of an event is taken to be the reconstructed vertex corresponding to the hardest scattering in the event, evaluated using tracking information alone, as described in Section 9.4.1 of Ref. [114].

The momentum resolution for electrons with a  $p_T \approx 45$  GeV from  $Z \rightarrow ee$  decays ranges from

1.6–5.0%. It is generally better in the barrel region than in the endcaps, and also depends on the bremsstrahlung energy emitted by the electron as it traverses the material in front of the ECAL [115, 116]. Electrons are identified with a multivariate analysis [117] discriminant that includes several quantities describing the track quality, the shape of the energy deposits in the ECAL, and the compatibility of the measurements from the tracker and the ECAL. Electrons must also pass a filter that rejects electrons coming from photon conversions and are required to be isolated [116]. Electrons are required to have  $p_T > 50$  GeV,  $|\eta| < 2.3$ , and be within a longitudinal distance  $d_z$  of 0.2 cm and a radial distance  $d_{xy}$  of 0.045 cm from the primary vertex (PV).

Matching muons to tracks measured in the silicon tracker results in a relative  $p_T$  resolution, for muons with  $p_T$  up to 100 GeV, of 1% in the barrel and 3% in the endcaps. The  $p_T$  resolution in the barrel is better than 7% for muons with  $p_T$  up to 1 TeV [118]. Muons are identified with requirements on the quality of the track reconstruction and on the number of measurements in the tracker and the muon system, and are required to be isolated [118]. Furthermore, muons must have  $p_T > 50$  GeV,  $|\eta| < 2.4$ , and be within a longitudinal distance  $d_z < 0.2$  cm and a radial distance  $d_{xy} < 0.045$  cm from the PV.

For each event, hadronic jets are clustered from reconstructed particles using the infrared- and collinear-safe anti- $k_T$  algorithm [119, 120] with a distance parameter of 0.4. Jet momentum is determined as the vectorial sum of all particle momenta in the jet, and is found from simulation to be, on average, within 5–10% of the true momentum over the entire  $p_T$  spectrum and detector acceptance. Pileup interactions can contribute additional tracks and calorimetric energy depositions to the jet momentum. To mitigate this effect, charged particles identified to be originating from pileup vertices are discarded and an offset correction is applied to correct for remaining contributions. Jet energy corrections are derived from simulation to bring the measured response of jets to that of particle level jets on average. In situ measurements of the momentum balance in dijet, photon + jet, Z + jet, and multijet events are used to account for any residual differences in the jet energy scale between data and simulation [121]. The jet energy resolution amounts typically to 15–20% at 30 GeV, 10% at 100 GeV, and 5% at 1 TeV [121]. Additional selection criteria are applied to each jet to remove jets potentially dominated by anomalous contributions from various subdetector components or reconstruction failures. In this analysis, jets are required to have  $p_T > 50$  GeV and  $|\eta| < 4.7$ , and must be separated from the selected leptons by  $\Delta R = \sqrt{(\Delta\eta)^2 + (\Delta\phi)^2} > 0.5$ , where  $\phi$  denotes the azimuthal angle.

Jets originating from the hadronization of b quarks are identified using the DEEPCSV algorithm [122, 123] based on a deep neural network with four hidden layers that is an extension of the combined secondary vertex algorithm [124]. It exploits observables related to the long lifetime and large mass of b hadrons. This analysis uses a fixed working point (WP) of DEEPCSV that corresponds to a 10% misidentification rate for jets originating from light quarks or gluons, and an efficiency of up to 90% in selecting b quark jets, depending on the jet  $p_T$  and  $\eta$ . The efficiency degrades to approximately 60% for  $p_T > 500$  GeV. In this analysis, b-tagged jets are required to have  $p_T > 50$  GeV and  $|\eta| < 2.4$  (2.5) for the 2016 (2017–2018) data-taking period.

Hadronic  $\tau$  lepton decays are reconstructed from jets, using the hadrons-plus-strips algorithm [125], which combines 1 or 3 tracks with energy deposits in the calorimeters, to identify the  $\tau$  lepton decay modes. Neutral pions are reconstructed as strips with dynamic size in  $\eta$ - $\phi$  from reconstructed electrons and photons, where the strip size varies as a function of the  $p_T$  of the electron or photon candidate. To distinguish genuine  $\tau_h$  decays from jets originating from the hadronization of quarks or gluons, electrons, or muons, the DEEPTAU algorithm [126] is used, which combines information from all individual reconstructed particles near the  $\tau_h$

candidate axis with properties of the  $\tau_h$  candidate and the event. The probability of a jet to be misidentified as a  $\tau_h$  candidate by the DEEPTAU algorithm depends on the  $p_T$  and quark flavor of the jet. In simulated  $W + \text{jets}$  events it has been estimated to be 0.43% for a genuine  $\tau_h$  identification efficiency of 70%. The misidentification rate for electrons (muons) is 2.60 (0.03)% for a genuine  $\tau_h$  identification efficiency of 80 (>99)%. Lastly, the  $\tau_h$  candidate is required to have  $p_T > 50 \text{ GeV}$ ,  $|\eta| < 2.3$ , and be within a longitudinal distance  $d_z$  of 0.2 cm from the PV.

The missing transverse momentum vector  $\vec{p}_T^{\text{miss}}$  is computed as the negative vector  $p_T$  sum of all the particle-flow candidates in an event, and its magnitude is denoted as  $p_T^{\text{miss}}$  [127]. The  $\vec{p}_T^{\text{miss}}$  is modified to account for corrections to the energy scale of the reconstructed jets in the event.

## 5 Event selection

This search targets a final state signature with energetic  $\tau$  leptons and b quark jets. Section 5.1 introduces a baseline event selection, which requires the events to be consistent with either the  $e\tau_h$ ,  $\mu\tau_h$ ,  $\tau_h\tau_h$ ,  $e\mu$ , or  $\mu\mu$  decay channel, where the electron, muon, or  $\tau_h$  object is assumed to be the visible product of  $\tau$  lepton decays. The most sensitive decay channels are  $e\tau_h$ ,  $\mu\tau_h$ , and  $\tau_h\tau_h$ , while the expected LQ signal contribution is negligible compared to the background in the  $e\mu$  and  $\mu\mu$  channels. However, the fully leptonic channels still provide a large sample of background events that help to constrain the systematic uncertainties in the simulated background in a combined fit. Event categories that target the resonant LQ production based on events with at least one high- $p_T$  jet not originating from a  $\tau_h$  decay are then defined in Section 5.2, and those targeting a nonresonant signal based on events with no such high- $p_T$  jets are defined in Section 5.3.

### 5.1 Baseline selection

This analysis makes use of three types of triggers depending on the explored final state. Events collected by single-electron triggers are considered in the  $e\tau_h$  channel, by single-muon triggers for the  $\mu\tau_h$ ,  $e\mu$ , and  $\mu\mu$  final states, and by triggers requiring a pair of  $\tau_h$  candidates for the  $\tau_h\tau_h$  channel. A minimum  $p_T$  of 27–35 GeV (24–27 GeV, 35–40 GeV) is required for each particle candidate to pass the single-electron (single-muon,  $\tau_h\tau_h$ ) triggers, varying between years of data taking. The  $\tau_h\tau_h$  triggers are limited to  $|\eta| < 2.1$ , therefore  $\tau_h$  candidates are required to have  $|\eta| < 2.1$  in the  $\tau_h\tau_h$  channel.

The  $e\tau_h$  ( $\mu\tau_h$ ) channel requires exactly one electron (muon) and at least one  $\tau_h$  candidate passing the reconstruction criteria described in Section 4. The selected lepton and  $\tau_h$  must have an angular separation of  $\Delta R > 0.5$  and have opposite-sign (OS) electric charge. If multiple such combinations of a lepton and a  $\tau_h$  candidate are found, the pair with the highest- $p_T$   $\tau_h$  candidate is selected. In order to reject background events from  $Z \rightarrow e^+e^-$  and  $Z \rightarrow \mu^+\mu^-$  decays, the DEEPTAU discriminators against leptons misidentified as  $\tau_h$  candidates are applied to the  $\tau_h$  object in both channels. In the  $e\tau_h$  ( $\mu\tau_h$ ) channel, the “Loose” (“V Loose”) WP of the discriminator against electrons, as defined in Ref. [126], is used. In both channels, the “V Loose” WP of the discriminator against muons is employed.

Lastly, for both the  $e\tau_h$  and  $\mu\tau_h$  channels, a veto on additional leptons is applied in order to reduce  $DY + \text{jets}$ ,  $t\bar{t}$ , and diboson backgrounds, as well as to keep orthogonality between the  $e\tau_h$  and  $\mu\tau_h$  channels. For this purpose, events with additional isolated electrons or muons that pass looser identification criteria are discarded.

Events in the  $\tau_h\tau_h$  channel are required to have two  $\tau_h$  candidates satisfying the criteria de-



tailed in Section 4. The two  $\tau_h$  candidates must be separated by  $\Delta R > 0.5$  and have OS electric charges as well. As in the case of the semileptonic channels, extra-lepton vetoes, and the DEEPTAU discriminators against leptons are applied. As there is little background in this channel from electrons or muons misidentified as  $\tau_h$  candidates, loose WPs of the discriminators against electrons (“VVLoose”) and muons (“VLoose”) are used.

In the  $e\mu$  ( $\mu\mu$ ) channel, the presence of exactly one electron and one muon (exactly two muons) of OS electric charges and with  $\Delta R > 0.5$  is required, while a veto is applied on additional leptons. The criteria discussed in Section 4 are applied.

## 5.2 Search for resonant LQ production

The final states of the single- and pair-production processes are characterized by two high- $p_T$   $\tau$  leptons and one or two high- $p_T$  b quarks. In order to obtain the highest sensitivity to the LQ signal, the event categorization and selections have been optimized. The kinematic variable showing the best separation power between signal and background is the scalar sum  $S_T^{\text{MET}}$  of the  $p_T$  of the  $\tau$  decay candidates ( $p_T^1, p_T^2$ ), the leading jet ( $p_T^j$ ), and  $p_T^{\text{miss}}$ ,

$$S_T^{\text{MET}} = p_T^1 + p_T^2 + p_T^j + p_T^{\text{miss}}. \quad (1)$$

The SM background has a steeply falling  $S_T^{\text{MET}}$  distribution, while the LQ signal is expected to appear at large values of  $S_T^{\text{MET}}$ . The signal strength is extracted from a simultaneous fit to the observed distribution of this observable. This analysis considers events that have at least one jet with  $p_T > 50$  GeV. Two orthogonal event categories are then constructed: the “0b” category, which requires zero loosely b-tagged jets with  $p_T > 50$  GeV, and the “ $\geq 1b$ ” category, which requires at least one such jet. The 0b category primarily targets events of single or pair production of LQs in which jets initiated by a b quark are not b tagged. An additional requirement is applied on the invariant mass  $m_{\text{vis}}$  of the sum of the four-momenta of all visible decay products of the two  $\tau$  leptons,  $m_{\text{vis}} > 100$  GeV, to remove DY events with negligible loss of signal.

The product of acceptance and efficiency for the vector LQ signal in the resonant signal categories 0b and  $\geq 1b$  is shown in the upper row of Fig. 2 as a function of  $m_{LQ}$ . The scalar LQ signal shows a very similar behavior. The acceptances and efficiencies are restricted to the sensitive region of  $S_T^{\text{MET}} > 800$  GeV and are computed with respect to all possible decay modes of the two  $\tau$  leptons. In the  $\tau_h\tau_h$  channel of the  $\geq 1b$  category, the product of acceptance and selection efficiency for the LQ pair production events varies with  $m_{LQ}$  between approximately 3.5 and 10.0%, while it varies between 1.0 and 7.5% for the single production. Below LQ masses of approximately 1 TeV, the acceptance and efficiency for resonant production decrease towards lower masses in the  $\geq 1b$  category because of a softer  $p_T$  spectrum. Contributions from the non-resonant signal are also considered in the 0b and  $\geq 1b$  categories, as one or more high- $p_T$  jets due to initial-state radiation or gluon splitting may be present.

## 5.3 Search for nonresonant LQ production

To increase the purity of the nonresonant signal, a small longitudinal Lorentz boost  $|\eta_1 + \eta_2|/2 < 1.1$  and a pseudorapidity difference  $|\Delta\eta| < 3$  between the two  $\tau$  decay candidates are required. To make this category orthogonal to those described in Section 5.2, selected events are required to have no jets with  $p_T > 50$  GeV. This category will therefore be referred to as the “0j” category. After these selections, the events are separated into three bins of the visible mass  $m_{\text{vis}}$ : 200–400, 400–600, and larger than 600 GeV, because the signal purity increases with  $m_{\text{vis}}$ .

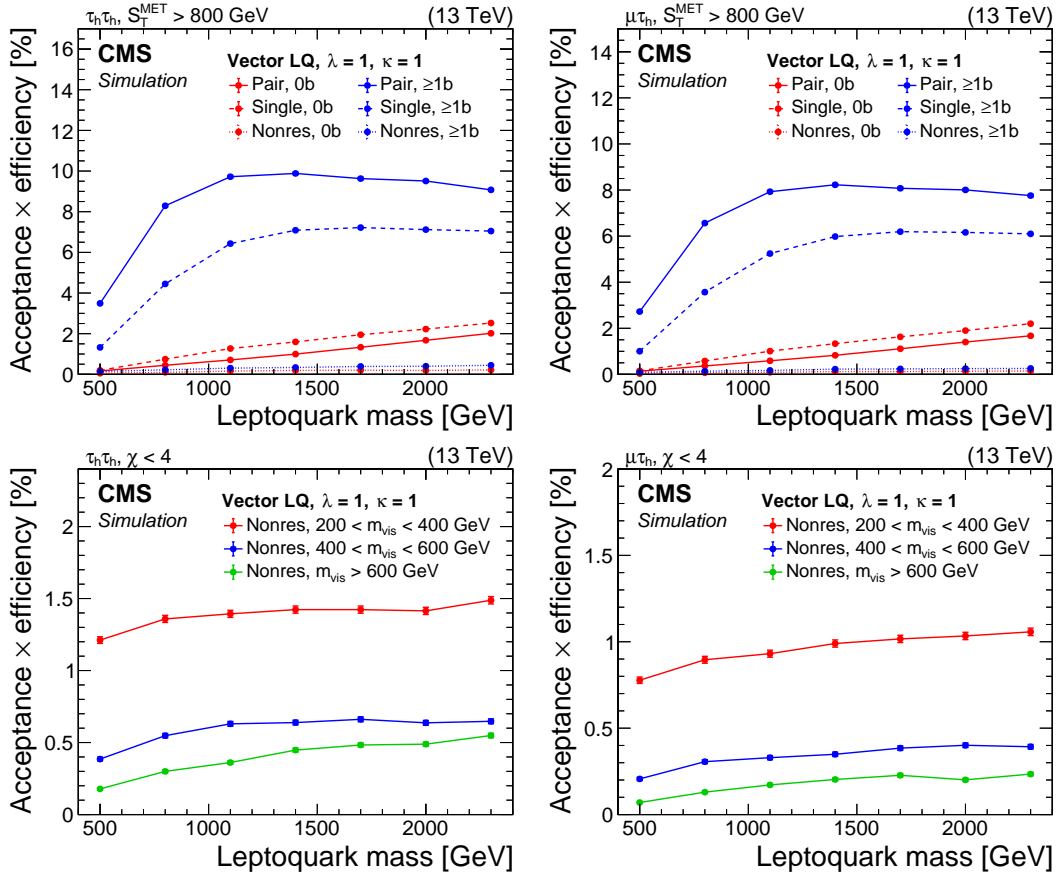


Figure 2: Product of acceptance and efficiency for a vector LQ signal in the  $\tau_h\tau_h$  (left) and  $\mu\tau_h$  (right) channels of the 0b and  $\geq 1b$  (upper), and the 0j categories (lower). The resonant LQ signals are neglected in the 0j category. Vertical bars (only just visible) indicate the statistical uncertainty.

In these three categories, the sensitive observable used for the signal extraction in a simultaneous fit is the angular separation between the two  $\tau$  lepton candidates, defined as  $\chi = \exp(|\Delta\eta|)$ . The choice of this variable is motivated by the fact that the  $\chi$  distribution in Rutherford scattering is flat [128], while new physics processes with a more isotropic angular distribution will appear as an excess at low  $\chi$  values. The  $\chi$  distribution is then measured over the range  $1 < \chi < 21$ , which implies a maximum value of  $|\Delta\eta| = 3.04$ .

The product of acceptance and efficiency for the vector LQ signal in the 0j categories is shown in the lower row of Fig. 2 as a function of  $m_{LQ}$ . Very similar behavior is found for the scalar LQ signal. The acceptances and efficiencies are restricted to the sensitive region of  $\chi < 4$  and are computed with respect to all possible decay modes of two  $\tau$  leptons.

## 6 Background estimation

For the search of a resonant LQ signal in the 0b and  $\geq 1b$  categories, the dominant backgrounds in most search channels stem from  $t\bar{t}$  production because of the presence of genuine electrons, muons,  $\tau$  leptons, and b quark jets from t quark decays. In final states with at least one  $\tau_h$  candidate, events with jets misidentified as  $\tau_h$  candidates ( $j \rightarrow \tau_h$  events) are another major source of background. For the nonresonant search in the 0j category, the main backgrounds in the signal region (SR) are DY production as well as the  $j \rightarrow \tau_h$  events.

The shape of the Z boson  $p_T$  spectrum of simulated DY + jets events is adjusted by simulation-to-data correction factors. These factors are derived as a function of the  $p_T$  of the selected dimuon system in a sample enriched with DY + jets dimuon events. This procedure is referred to as “Z boson  $p_T$  reweighting” in the following.

### 6.1 Background estimation for the $\ell\tau_h$ and $\tau_h\tau_h$ channels

For the  $e\tau_h$ ,  $\mu\tau_h$ , and  $\tau_h\tau_h$  channels, all SM background processes are estimated using simulation, except for background of  $j \rightarrow \tau_h$  events. The  $j \rightarrow \tau_h$  background in the different signal channels consists of QCD multijet, W + jets, and  $t\bar{t}$  events. This background is estimated with the so-called “fake-factor” (FF) method that is described in detail in Refs. [129, 130]. Depending on the event category, the  $j \rightarrow \tau_h$  background constitutes approximately 25–71% of the total background in the  $e\tau_h$  and  $\mu\tau_h$  channels and 46–82% in the  $\tau_h\tau_h$  channel, decreasing with the number of b-tagged jets and the minimum requirement imposed on  $m_{\text{vis}}$ .

The FF method proceeds by defining an application region (AR) containing the same selection criteria as in the SR, with the exception that the requirement on the DEEPTAU discriminator against jets is inverted for one  $\tau_h$  candidate, while still requiring it to pass the “VLoose” WP. The AR is primarily populated by events with jets misidentified as  $\tau_h$  candidates, and has contamination from genuine  $\tau_h$  decays at the level of a few percent or below. The FF represents the ratio of the number of events with a jet misidentified as a  $\tau_h$  candidate in the AR to that in the SR. For both the AR and SR, corresponding control regions (CRs) are defined, in which the same requirements on the DEEPTAU discriminator against jets as in the AR and SR are applied. The FF is measured in data as the ratio of the number of events in each of the two CRs, in which a jet was misidentified as a  $\tau_h$  candidate.

The FF is measured separately for the three dominant background processes using dedicated CRs that are pure in the respective background in order to take into account the differing compositions of jet flavors. The FFs for QCD multijet events are estimated in a CR with same-sign (SS)  $\tau_h$  pairs, while the FFs for W + jets events are estimated in  $\ell\tau_h$  final states with no b-tagged jets and a high transverse mass  $m_T$  of the lepton and  $\vec{p}_T^{\text{miss}}$ . The transverse mass is defined as  $m_T = \sqrt{2p_T^\ell p_T^{\text{miss}} (1 - \cos \Delta\phi)}$ , where  $\Delta\phi$  denotes the azimuthal distance between the lepton and  $\vec{p}_T^{\text{miss}}$ . For  $t\bar{t}$  events, the FF are estimated purely from simulated samples. The FFs measured separately for the three background processes are combined in a weighted sum, in which each FF is weighted with the fraction of events of the corresponding process in the AR. The  $j \rightarrow \tau_h$  background in the SR is obtained by applying the combined FF to the data in the AR, from which simulated events with genuine  $\tau_h$  candidates have been subtracted. The combined FF takes an average value between 0.40 and 0.47, depending on the category.

The FF is calculated as a function of the  $p_T$  of the  $\tau_h$  candidate and the number of jets in the event. In  $\ell\tau_h$  events, the FF is also measured as a function of the  $\Delta R$  between the  $\tau_h$  candidate and the light lepton. A polynomial function is fitted to the FF values as a function of  $p_T$  to interpolate between measured values. The presence of small backgrounds in the AR that contain genuine  $\tau_h$  decays results in an underestimation of the number of events with a misidentified  $\tau_h$  in the SR of up to 2%. Therefore, a correction is applied based on the fractions of these processes in simulated events. Corresponding uncertainties are incorporated into the fit model of the SR, as described in Section 7. The FF method for the  $\tau_h\tau_h$  channel is similar, with the exception that a weight factor of 0.5 is applied to take into account combinatorial effects due to the presence of two  $\tau_h$  candidates.

The FF method is tested in two validation regions (VRs): one is constructed by inverting the leading jet  $p_T$  requirement (i.e.,  $p_T < 50$  GeV) and the other by using events with two  $\tau_h$  can-

didates that do not fulfill the DEEPTAU identification requirement against jets used to define the SR. For both VRs, all other selection criteria are kept identical to the SR, except that the b tagging requirement is removed to increase the number of events. The signal contamination is negligible in both VRs. Data and the predicted background are found to agree within statistical uncertainties, demonstrating the validity of the FF method.

## 6.2 Background estimation for the $e\mu$ and $\mu\mu$ channels

In the  $e\mu$  and  $\mu\mu$  channels, all SM background processes, except for the QCD multijet background, are estimated using simulation and normalized according to the theoretical cross sections.

The QCD multijet background is small and is estimated from an SS CR. In this CR, the QCD multijet background shape is constructed by subtracting the simulated SM backgrounds from observed data in each histogram bin. This shape is scaled by an extrapolation factor to obtain the expected QCD multijet background in the OS SR. The extrapolation factor is measured in simulated QCD multijet events by inverting the lepton isolation requirement, and is found to be approximately 2.4.

## 7 Systematic uncertainties

Various systematic uncertainties are taken into account as nuisance parameters in the final fit of the expected background and signal to the data. Uncertainties are treated differently depending on whether they affect only the rate of a given process or both its rate and shape in the distributions used in the final fit.

### 7.1 Rate uncertainties

The uncertainty in the integrated luminosity varies depending on the year [131–133], amounting to 1.6% for the 2016–2018 sample, and affects the rate of the signal and background processes that are based on simulation. Uncertainties in the electron or muon identification and trigger efficiency amount to 2% each [134]. For events in which electrons or muons are misidentified as  $\tau_h$  candidates, predominantly  $Z \rightarrow e^+e^-$  events in the  $e\tau_h$  channel and  $Z \rightarrow \mu^+\mu^-$  events in the  $\mu\tau_h$  channel, rate uncertainties of 12 and 25% [135], respectively, are applied, as determined via the “tag-and-probe” method [136].

The QCD multijet background estimation in the  $e\mu$  and  $\mu\mu$  channels is found to have rate uncertainties up to 20%. The uncertainty in the  $DY + \text{jets}$  cross section in the  $\geq 1b$  category is estimated using a dedicated CR of events with two  $\tau_h$  candidates and at least one b-tagged jet and  $m_{\text{vis}} < 100 \text{ GeV}$ . A 20% uncertainty is assigned to the  $DY + \text{jets}$  cross section in the  $\geq 1b$  category based on the total number of observed data events compared to the expected background in this CR. In the other signal categories, the uncertainty in the NNLO computation is given as 3%. The uncertainties in the cross section for the  $t\bar{t}$ , diboson, and single t quark processes are 5.5, 6, and 5.5%, respectively. A value of 5, 10, and 25% is assigned to the uncertainty in the cross section for  $V\gamma + \text{jets}$ , electroweak W or Z boson, and triboson production, respectively. These uncertainties are correlated between the years but assumed to be uncorrelated between 0j and the other signal categories.

### 7.2 Shape uncertainties

Differences in the  $\tau_h$  identification efficiency between data and simulation are corrected by scale factors (SFs) that are applied as functions of the  $\tau_h$  decay mode for the  $\tau_h\tau_h$  channel.

The uncertainty in these SFs is predominantly statistical and assumed to be uncorrelated between the three data-taking years and the four  $\tau_h$  decay modes considered. In the  $\mu\tau_h$  and  $e\tau_h$  channels instead, an inclusive SF is applied for each year, and its uncertainty is assumed as uncorrelated between the three years but fully correlated between both channels. An additional uncertainty, fully correlated between all analysis regions, is assigned to account for the extrapolation of each  $\tau_h$  identification SF from  $p_T = 40$  GeV to higher values, covering a potential  $p_T$ -dependence of the SFs. The uncertainty is expanded linearly up to values of +8 and -17% at  $p_T = 500$  GeV, beyond which it is continued as a constant. The uncertainty in the trigger efficiency SF in the  $\tau_h\tau_h$  channel is taken into account by varying the SF within its total uncertainty. This uncertainty is considered uncorrelated across years and fully correlated between event categories in the  $\tau_h\tau_h$  channel.

The uncertainty in the  $\tau_h$  energy scale depends on the  $\tau_h$  decay mode and  $p_T$ , and varies between 0.6–1.4% for  $p_T < 34$  GeV, and between 1–4% for  $p_T > 170$  GeV, with a linear interpolation between the respective uncertainties for  $34 < p_T < 170$  GeV. It is only applied to the simulated events with genuine  $\tau_h$  candidates, namely those in DY + jets,  $t\bar{t}$ , and LQ events. It is uncorrelated between the years but correlated between the different channels. For events in which a muon is misidentified as a  $\tau_h$  candidate, a shape uncertainty is derived by varying the  $\tau_h$  energy scale by 1%. For events with electrons that are misidentified as a  $\tau_h$  candidate, the uncertainties in the measured energy corrections are used, which vary from 0.8 to 6.6% depending on the  $\tau_h$  decay mode and pseudorapidity region.

The uncertainties in the jet energy scale are up to 4%, depending on the values of  $p_T$  and  $\eta$  of the jet [137]. The uncertainties in the jet energy scale and resolution are taken into account as shape uncertainties by taking the one-standard-deviation variations of the corrections and propagating them to all the affected variables in the analysis (including jet  $p_T$ , jet multiplicity, b tag multiplicity,  $p_T^{\text{miss}}$  and  $S_T^{\text{MET}}$ ). These uncertainties are assumed to be uncorrelated between the years and correlated between the three signal categories and different  $\tau$  decay channels. The uncertainty in the correction of the ECAL timing shift at the trigger level is taken into account by varying the correction factor within its uncertainties.

The uncertainties in the b tagging efficiency of heavy-flavor jets (b and c quark jets) and the misidentification rate of light-flavor (u, d, s quarks) and gluon jets are propagated from the uncertainties in the b tagging SFs. The efficiencies for b and c quarks are assumed to be correlated, as are the misidentification rates for light-flavor and gluon jets. Most of the shape variations have little dependence on  $S_T^{\text{MET}}$ , with about a 1% change in overall yield in the  $\geq 1b$  category, and less than 3% in 0b. The uncertainties are partially correlated between the years.

The uncertainties related to the FF method include the total systematic uncertainty in the measurement of the FFs in each of the W + jets,  $t\bar{t}$ , and QCD CRs, as well as the statistical uncertainty in the  $p_T$ -interpolation of the FFs. They are treated as uncorrelated between the years, event categories, and  $\tau\tau$  final states, as the dominant background process can differ and the FF measurement is dominated by the statistical uncertainty due to the limited number of events in the CRs. In addition, the statistical uncertainty in the FF interpolation is considered uncorrelated between four bins in  $\tau_h p_T$  (<100, 100–200, 200–500, >500 GeV) to allow independent variations of the FFs in regions with different kinematic properties.

The uncertainty in the Z boson  $p_T$  reweighting is conservatively estimated by varying the simulation-to-data correction factors up and down by 50%. Similarly, an uncertainty is assigned to the modeling of the t quark  $p_T$  in simulated  $t\bar{t}$ , which was found to differ between data and simulation [138–140]. Distributions of  $S_T^{\text{MET}}$  and  $\chi$  with differing shapes are created by applying corrections to the simulated t quark  $p_T$  distribution of the form described in Sec-

tion 3 of Ref. [141] but with a much larger range of variations in order to ensure that the final fit is only weakly constrained by this uncertainty. Owing to large pre-fit uncertainties, the Z boson and t quark  $p_T$  distributions are modeled using data in the  $e\mu$  and  $\mu\mu$  regions in the final maximum likelihood fit.

The renormalization and factorization scales  $\mu_R$  and  $\mu_F$  used in the event generation depend on the process simulated and the generator used. They are either set to fixed values or are related to kinematic properties of the individual generated events. The shape uncertainties due to these scales are obtained by varying  $\mu_R$  and  $\mu_F$  simultaneously by the same or a different factor (0.5, 1, or 2) while keeping the total yield constant and taking the envelope of all variations. Extreme combinations of  $(\mu_R, \mu_F)$  varied by factors of (0.5, 2) or (2, 0.5) are excluded. Similarly, the shape uncertainties due to the PDFs are taken into account by creating a symmetric envelope [142].

Finally, uncertainties related to the limited number of simulated events are taken into account with the Barlow–Beeston-lite approach [143, 144]. They are considered for all bins of the distributions that are used to extract the results. They are uncorrelated across the different samples and across the bins of a single distribution.

All systematic uncertainties are summarized in Table 1. In addition to the statistical uncertainty due to the limited size of the simulated samples, the systematic uncertainties in the identification of genuine  $\tau_h$  candidates and in the estimation of the  $j \rightarrow \tau_h$  contribution from data in CRs have the dominant impact on the expected sensitivity of this search.

## 8 Results

A binned maximum likelihood fit [145] of the observed  $S_T^{\text{MET}}$  and  $\chi$  distributions in all channels, event categories, and data-taking periods is used to search for a possible signal over the expected background. The nuisance parameters assigned to systematic uncertainties in the normalization of the distributions are modeled with log-normal probability distributions in the fit. Nuisance parameters for uncertainties affecting the shape of a distribution are modeled with Gaussian distributions. In addition to searching for each LQ production mechanism separately, results for the combined LQ signal with a total cross section  $\sigma^{\text{tot}}$  are also presented.

Figure 3 shows representative postfit distributions of  $S_T^{\text{MET}}$  in the  $\tau_h\tau_h$ ,  $\ell\tau_h$ , and  $e\mu$  channels in the 0b and  $\geq 1b$  categories, while Fig. 4 shows the postfit distributions of  $\chi$  in the  $400 < m_{\text{vis}} < 600$  and  $m_{\text{vis}} > 600$  GeV bins of the 0j category. The total vector LQ signal for the benchmark  $m_{\text{LQ}} = 2000$  GeV with  $\lambda = 2.5$  and  $\kappa = 1$  is overlaid and normalized to the best-fit cross section. The binning of all histograms is chosen such that the total statistical uncertainty in the SM background expectation of a given bin does not exceed 20%.

The postfit event yields of the signal and backgrounds are compared to the observed data in Table 2 for  $\tau\tau$  final states with at least one  $\tau_h$ , which are most sensitive to the LQ signal, and all event categories considered in the fit. Table 3 shows the best-fit signal cross section with the corresponding local significance for different LQ production modes. For lower masses and coupling strengths  $\lambda$ , the observed data agree with the SM expectation within approximately one standard deviation, and within two standard deviations for  $\lambda < 1.5$  and all LQ masses considered. At higher masses and coupling strengths, however, an excess with a local significance of up to 2.8 standard deviations above the SM background expectation is found. The significance is computed using the ratio of the profile likelihood of the background-only fit to that of the fit in which the normalization of the total signal is a free parameter [146]. This ex-

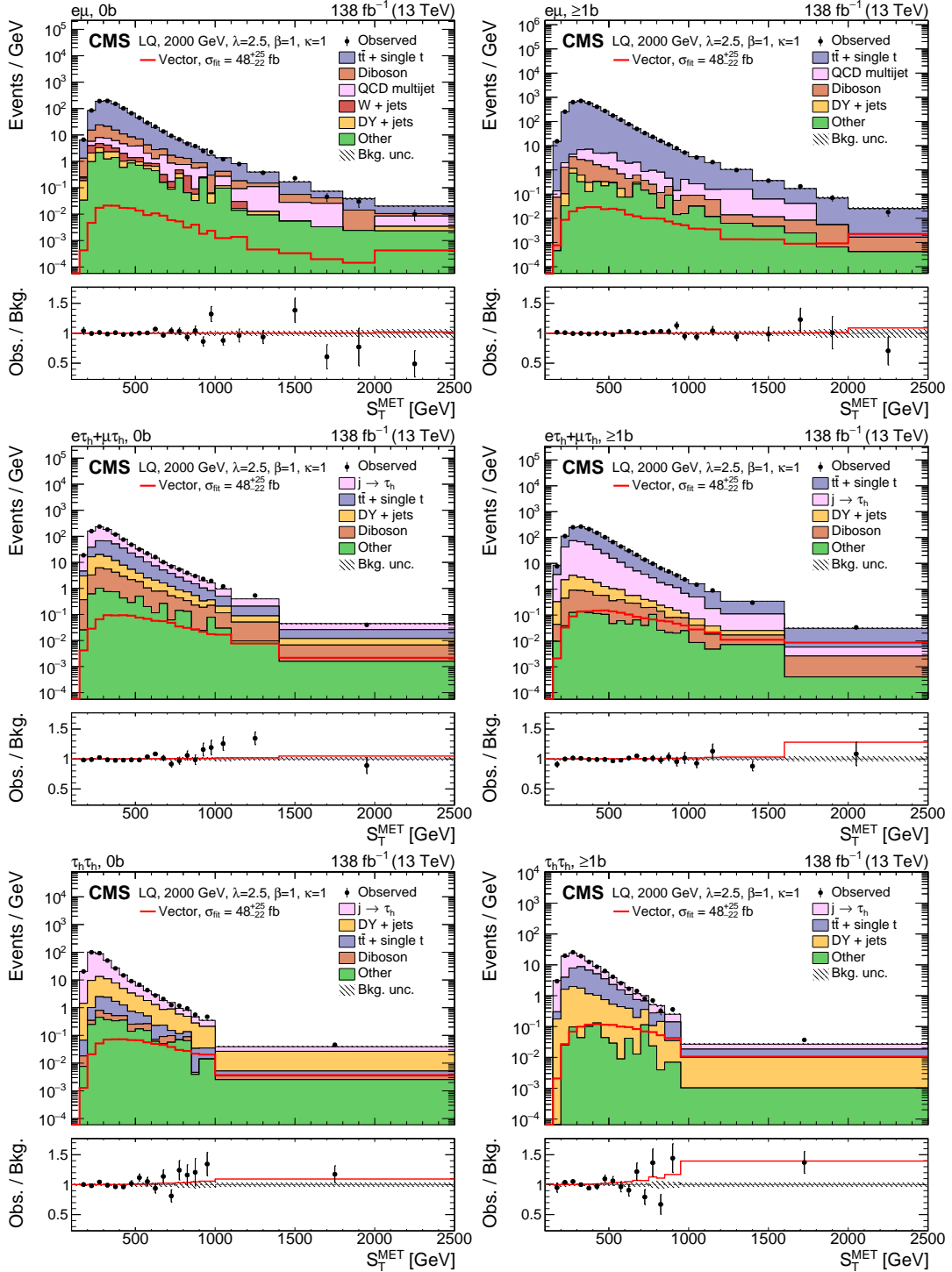


Figure 3: Postfit distributions of  $S_T^{\text{MET}}$  for the combined 2016–2018 data set after a simultaneous fit of the background and vector LQ signal to the data. The last bin includes the overflow. The  $e\mu$  (top),  $e\tau_h$  (center), and  $\tau_h\tau_h$  (bottom) channels in the 0b (left) and  $\geq 1b$  (right) categories are shown. The fitted signal distribution for the total vector LQ signal (red line) with a mass of 2000 GeV,  $\lambda = 2.5$ , and  $\kappa = 1$  is overlaid. In each distribution, the lower panel shows the ratio of the data (black markers) or the sum of the postfit signal and background (red line) to the postfit background. The hatched band indicates the total postfit uncertainty in the background.

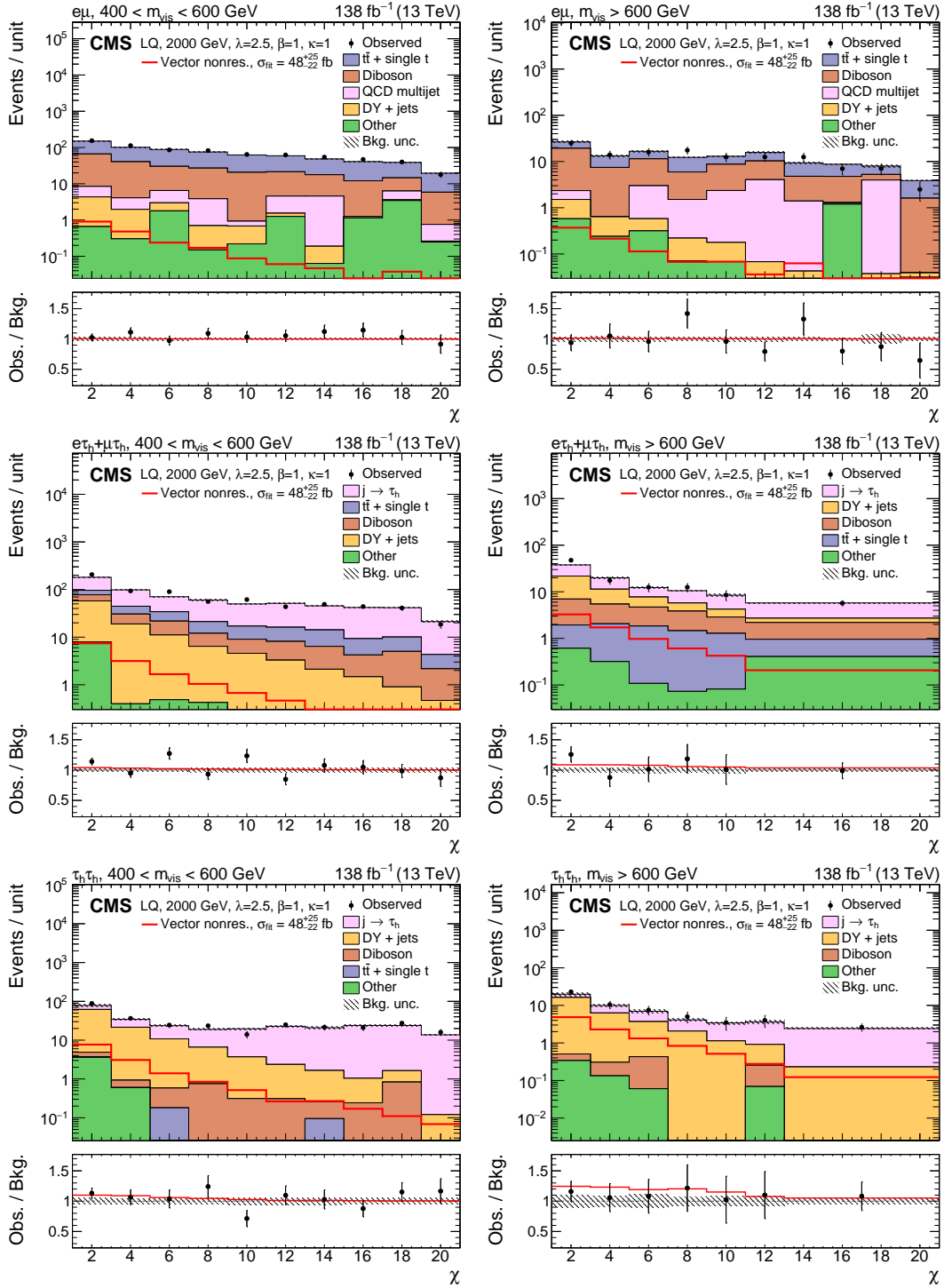


Figure 4: Postfit distributions of  $\chi$  for the combined 2016–2018 data set after a simultaneous fit of the background and vector LQ signal to the data. The last bin includes the overflow. The  $e\mu$  (top),  $\ell\tau_h$  (center), and  $\tau_h\tau_h$  (bottom) channels in the  $400 < m_{\text{vis}} < 600$  GeV (left) and  $m_{\text{vis}} > 600$  GeV (right) categories are shown. The fitted signal distribution for the nonresonant vector LQ model (red line) with a mass of 2000 GeV,  $\lambda = 2.5$ , and  $\kappa = 1$  is overlaid. The contribution from resonant LQ production is neglected. In each distribution, the lower panel shows the ratio of the data (black markers) or the sum of the postfit signal and background (red line) to the postfit background. The hatched band indicates the total postfit uncertainty in the background.



Table 1: The sources of uncertainty considered, categorized as to whether they affect the rate or shape of the distributions. “s.d.” refers to the standard deviation of the input variable and “(mis)ID” stands for “(mis)identification”.

Source	Channel				
	$e\tau_h$	$\mu\tau_h$	$\tau_h\tau_h$	$e\mu$	$\mu\mu$
<i>Rate</i>					
Integrated luminosity			1.2–2.5%		
Electron ID	2%	—	—	2%	—
Electron trigger	2%	—	—	—	—
Muon ID	—	2%	—	2%	2%
Muon trigger	—	2%	—	2%	2%
e misID as $\tau_h$	12%	—	12%	—	—
$\mu$ misID as $\tau_h$	—	25%	25%	—	—
QCD multijet	—	—	—	20%	20%
W + jets cross section	—	—	—	6%	6%
DY + jets cross section		20% in $\geq 1b$ , 3% otherwise			
$t\bar{t}$ cross section			5.5%		
Diboson cross section			6%		
Single t quark cross section			5.5%		
$V\gamma$ + jets cross section			5%		
Electroweak W/Z boson cross section			10%		
Triboson cross section			25%		
Jet energy scale			5% in 0j		
$p_T^{\text{miss}}$ scale			Up to 4%		
<i>Shape</i>					
$\tau_h$ trigger	—	—	$\pm 1$ s.d. in the SF	—	—
$\tau_h$ ID efficiency	$\pm 1$ s.d. in SF, $p_T$ extrapolation			—	—
$\tau_h$ energy scale	$\pm 1$ s.d. on the energy scale			—	—
Energy scale $\mu$ misID as $\tau_h$	$\pm 1\%$ on the energy scale			—	—
Energy scale e misID as $\tau_h$	$\pm 1$ s.d. on the energy scale			—	—
FF shape variations	Syst. shape variations			—	—
b tagging efficiency	$\pm 1$ s.d. in b tagging SFs				
b tagging mistag rate	$\pm 1$ s.d. in b tagging SFs				
Jet energy scale	$\pm 1$ s.d. in SF in 0b, $\geq 1b$				
Jet energy resolution	$\pm 1$ s.d. in SF in 0b, $\geq 1b$				
ECAL trigger timing	$\pm 1$ s.d. in SF				
PDF variations	Envelope of PDF variations				
$\mu_R$ & $\mu_F$ variations	Envelope of scale variations				
Z boson $p_T$ reweighting	Weight applied $\pm 50\%$				
t quark $p_T$ reweighting	Ref. [141] with larger variations				

cess is observed across several channels, as well as in both the  $\chi$  and  $S_T^{\text{MET}}$  distributions in the different jet categories. The excess is most prominent for the nonresonant signal in the analysis, which contributes to the combined excess increasingly at larger LQ masses and couplings. The significance of the nonresonant signal by itself has no strong dependence on  $m_{\text{LQ}}$  or  $\lambda$ , hence the look-elsewhere effect is negligible for the nonresonant signal. When combined with the pair and single production contributions to the total LQ signal, the excess at lower LQ masses and couplings becomes less significant.

Table 2: Event yields of data as well as signal and background after the combined fit to the data in  $\tau\tau$  final states with at least one  $\tau_h$ . The vector LQ benchmark with  $m_{LQ} = 2000$  GeV,  $\lambda = 2.5$ , and  $\kappa = 1$  is used as signal and normalized to the best-fit cross section of  $\sigma_{\text{fit}} = 48_{-22}^{+25}$  fb. The uncertainties reported are the total postfit uncertainties.

Category	Channel	Data	Signal	Total bkg.	$t\bar{t}$ + single t	DY + jets	Diboson	$j \rightarrow \tau_h$	Other
0b	$\ell\tau_h$	47277	52 ± 24	47280 ± 240	12100 ± 160	3225 ± 95	1298 ± 71	30380 ± 300	275 ± 17
	$\tau_h\tau_h$	16757	42 ± 17	16670 ± 180	389 ± 14	2480 ± 100	75 ± 4	13590 ± 200	134 ± 8
$\geq 1b$	$\ell\tau_h$	65810	92 ± 44	65780 ± 280	48160 ± 380	641 ± 31	271 ± 18	16650 ± 370	58 ± 6
	$\tau_h\tau_h$	5428	77 ± 35	5328 ± 82	1644 ± 57	512 ± 26	—	3139 ± 98	33 ± 4
$m_{\text{vis}} < 200$ GeV	$\ell\tau_h$	24324	81 ± 39	24220 ± 170	3478 ± 75	2068 ± 42	1350 ± 72	17200 ± 170	114 ± 7
	$\tau_h\tau_h$	16357	67 ± 29	16290 ± 150	113 ± 5	2112 ± 88	52 ± 3	13940 ± 160	72 ± 5
$m_{\text{vis}} \in [400, 600]$ GeV	$\ell\tau_h$	1407	31 ± 14	1331 ± 33	182 ± 9	195 ± 6	142 ± 8	793 ± 33	20 ± 4
	$\tau_h\tau_h$	596	29 ± 13	561 ± 23	1 ± 0	205 ± 13	9 ± 1	337 ± 19	8 ± 3
$m_{\text{vis}} > 600$ GeV	$\ell\tau_h$	254	16 ± 7	234 ± 11	20 ± 2	59 ± 3	43 ± 3	106 ± 8	6 ± 2
	$\tau_h\tau_h$	128	21 ± 9	114 ± 10	—	60 ± 6	2 ± 0	52 ± 8	1 ± 0

Table 3: Best-fit LQ cross sections  $\sigma_{\text{fit}}$  for various masses and coupling strengths  $\lambda$ , and the corresponding local significance  $z$  (given in standard deviations) for different production modes individually, as well as their combination. The look-elsewhere effect is negligible.

Signal	$m_{\text{LQ}} = 1400 \text{ GeV}$		$m_{\text{LQ}} = 2000 \text{ GeV}$	
	$\sigma_{\text{fit}} [\text{fb}]$	$z$	$\sigma_{\text{fit}} [\text{fb}]$	$z$
<i>Scalar</i>				
Pair	$0.46^{+0.51}_{-0.49}$	1.0	$0.39^{+0.45}_{-0.43}$	0.9
Single, $\lambda = 1$	$1.32^{+1.03}_{-0.99}$	1.3	$0.84^{+0.73}_{-0.70}$	1.2
Single, $\lambda = 2.5$	$8.7^{+6.0}_{-5.7}$	1.5	$17^{+12}_{-11}$	1.5
Nonres.	$92^{+44}_{-38}$	2.8	$83^{+39}_{-34}$	2.8
Total, $\lambda = 1$	$2.3^{+2.1}_{-2.0}$	1.2	$10.3^{+7.1}_{-6.4}$	1.6
Total, $\lambda = 2.5$	$47^{+25}_{-22}$	2.4	$78^{+37}_{-32}$	2.8
<i>Vector, <math>\kappa = 0</math></i>				
Pair	$0.46^{+0.51}_{-0.48}$	1.0	$0.41^{+0.44}_{-0.42}$	1.0
Single, $\lambda = 1$	$1.20^{+0.96}_{-0.92}$	1.3	$0.81^{+0.71}_{-0.68}$	1.2
Single, $\lambda = 2.5$	$19^{+13}_{-12}$	1.6	$31^{+22}_{-22}$	1.5
Nonres.	$71^{+34}_{-29}$	2.8	$62^{+30}_{-26}$	2.7
Total, $\lambda = 1$	$1.8^{+1.7}_{-1.6}$	1.1	$8.2^{+5.7}_{-5.2}$	1.6
Total, $\lambda = 2.5$	$47^{+24}_{-21}$	2.5	$62^{+31}_{-26}$	2.7
<i>Vector, <math>\kappa = 1</math></i>				
Pair	$0.46^{+0.51}_{-0.48}$	1.0	$0.41^{+0.44}_{-0.42}$	1.0
Single, $\lambda = 1$	$1.20^{+0.96}_{-0.92}$	1.3	$0.81^{+0.71}_{-0.68}$	1.2
Single, $\lambda = 2.5$	$9.8^{+7.0}_{-6.7}$	1.5	$24^{+19}_{-18}$	1.3
Nonres.	$71^{+34}_{-29}$	2.8	$62^{+30}_{-26}$	2.7
Total, $\lambda = 1$	$0.72^{+0.75}_{-0.72}$	1.0	$1.8^{+1.6}_{-1.5}$	1.2
Total, $\lambda = 2.5$	$12.5^{+8.3}_{-7.5}$	1.7	$48^{+25}_{-22}$	2.5

To better understand the origin of the excess and how compatible the signal model is with each different final state, the fit of the total LQ signal is performed again, but with one independent signal normalization parameter in each of the three jet categories (0j, 0b,  $\geq 1b$ ) while keeping common nuisance parameters. For each fitted cross section, a significance is computed while leaving the other two signal normalization parameters freely floating. For the  $m_{LQ} = 2000$  GeV,  $\lambda = 2.5$  benchmark, which yields the largest combined excess, the local significances in the 0j and  $\geq 1b$  categories range from 2.5 to 3.2 and 1.8 to 2.0 standard deviations, respectively, depending on the spin of the LQ and the coupling parameter  $\kappa$ . In the 0b category, a local significance between 3.4 and 3.7 standard deviations is found for the scalar and vector LQ models.

In a search performed by the ATLAS Collaboration [77], the LQ benchmark used in this analysis has been excluded, warranting the study of alternative signal models as a potential explanation of the results. As can be seen in Fig. 3, the largest excess of events is observed in the 0b category at high values of  $S_T^{MET}$  and most prominently in the  $\ell\tau_h$  channel, which is not expected for the model with exclusive LQ-b- $\tau$  couplings considered in this analysis. An improved description of the data could be possible with additional LQ couplings to particles of lighter generations. An independent analysis group based on Ref. [147] finds consistent results when applying similar event categorization and selection. A detailed study of events in the 0b category with  $S_T^{MET} > 800$  GeV excluded detector-level and reconstruction issues as a cause of the excess. This study also led to an improved modeling of the background due to jets misidentified as  $\tau_h$  objects with high  $p_T$  in this analysis, and the systematic uncertainties associated with genuine and misidentified  $\tau_h$  candidates. However, the excess was found to be robust against alternative  $\tau_h$  uncertainty models such as modified correlation schemes or different parametrizations of the uncertainties.

We set upper limits on the cross section of single, pair, and nonresonant production, as well as their sum, using a profile likelihood ratio test statistic and the  $CL_s$  criterion [148, 149]. The distributions of the test statistic are determined analytically using asymptotic approximations [146]. All limits are placed under the assumption of LQs coupling exclusively to b quarks and  $\tau$  leptons ( $\beta = 1$ ). The single production cross section approximately scales with  $\lambda^2$  at lower values of  $\lambda < 1.5$ , while the nonresonant production cross section is proportional to  $\lambda^4$ . Consequently, an upper limit on the total cross section  $\sigma^{tot}$  can be derived for different values of  $\lambda$ . To exclude regions of the  $\lambda$ - $m_{LQ}$  parameter space, the upper limit on  $\lambda$  at the 95% CL is computed by varying  $\lambda$ . The observed and expected upper limits at the 95% CL on the total cross section of scalar and vector LQ production are shown in Figs. 5 and 6, respectively, for  $\lambda = 1$  and 2.5.

Figures 7 and 8 show the upper limit on  $\lambda$  at the 95% CL as a function of  $m_{LQ}$  for the scalar and vector model. They include one line for each production mode, as well as their combination, which allows for the exclusion of a larger region at higher values of  $\lambda$ , where the single and nonresonant production start to contribute more significantly. Figure 9 shows the upper limit on the coupling strength for LQs exchanged in the  $t$  channel with an extended coupling range, placing constraints on LQs with masses and coupling strengths of up to 3 TeV and 3.5, respectively. The region with blue shading shows the parameter space preferred by one of the models proposed to explain the B physics anomalies [61]. At 95% confidence level, LQ masses below 1.22 TeV are excluded for the scalar model with  $\lambda = 1$ , and below 1.50 (1.82) TeV for the vector model with  $\lambda = 1$  and a coupling parameter  $\kappa = 0(1)$ . At  $\lambda = 2.5$ , the lower limits are 1.31 TeV for a scalar model, and 1.73 (1.88) TeV for a vector model with  $\kappa = 0(1)$ .

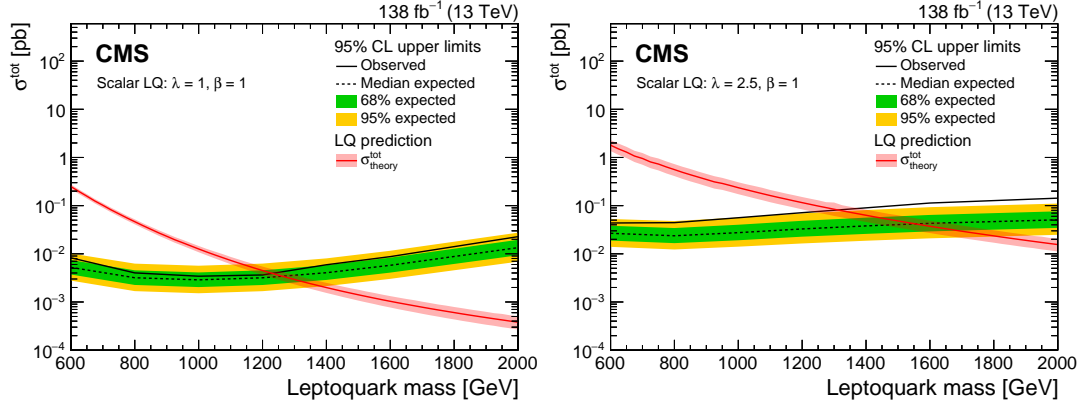


Figure 5: Observed and expected upper limit on the total cross section of a scalar LQ signal with  $\lambda = 1$  (left) and  $2.5$  (right) at the 95% CL under the assumption of exclusive LQ couplings to  $b$  quarks and  $\tau$  leptons. The inner (green) band and the outer (yellow) band indicate the regions containing 68 and 95%, respectively, of the distribution of limits expected under the background-only hypothesis. The red line shows the cross section with the shaded band indicating the theoretical uncertainties.

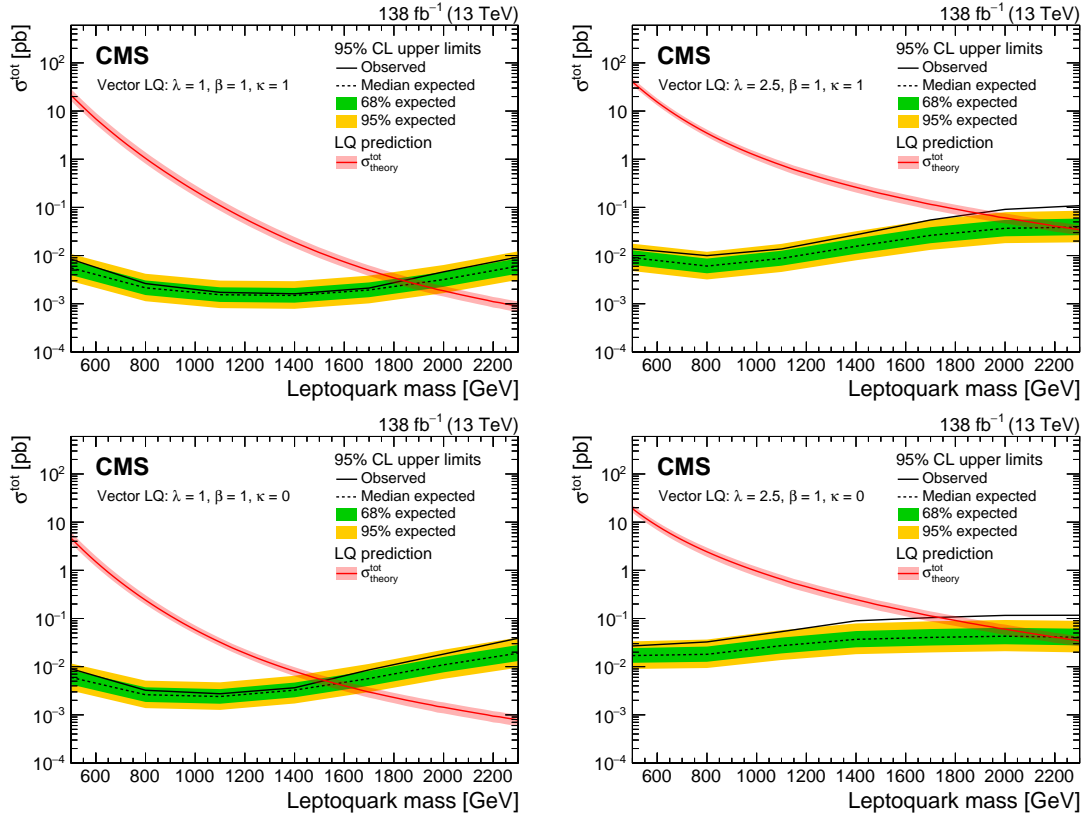


Figure 6: Observed and expected upper limit on the total cross section of a vector LQ signal with  $\lambda = 1$  (left) and  $2.5$  (right) at the 95% CL under the assumption of exclusive LQ couplings to  $b$  quarks and  $\tau$  leptons. The upper (lower) row assumes a coupling parameter  $\kappa = 1$  ( $0$ ). The inner (green) band and the outer (yellow) band indicate the regions containing 68 and 95%, respectively, of the distribution of limits expected under the background-only hypothesis. The red line shows the cross section calculated at LO with the shaded band indicating the theoretical uncertainties.

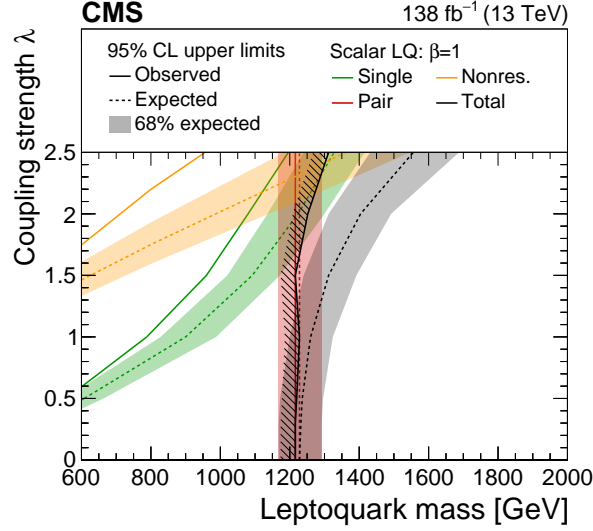


Figure 7: Observed and expected upper limit at the 95% CL on the coupling strength  $\lambda$  of a scalar LQ under the assumption of exclusive LQ couplings to  $b$  quarks and  $\tau$  leptons. The limits derived for the single (green), pair (red), nonresonant (orange), and total LQ production (black) are shown. The shaded bands around the expected limit lines correspond to the regions containing 68% of the distribution of limits expected under the background-only hypothesis. The hatches indicate the excluded side of the parameter space with respect to the combined observed limit.

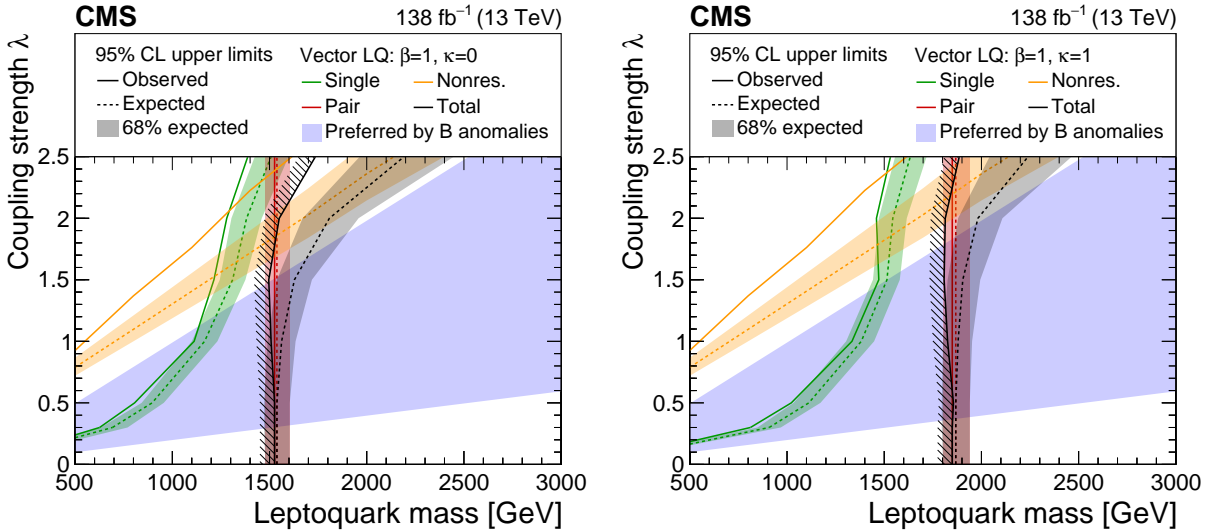


Figure 8: Observed and expected upper limit at the 95% CL on the coupling strength  $\lambda$  of a vector LQ model with  $\kappa = 0$  (left) and  $\kappa = 1$  (right) under the assumption of exclusive LQ couplings to  $b$  quarks and  $\tau$  leptons. The limits derived for the single (green), pair (red), nonresonant (orange), and total LQ production (black) are shown. The shaded bands around the expected limit lines correspond to the regions containing 68% of the distribution of limits expected under the background-only hypothesis. The hatches indicate the excluded side of the parameter space with respect to the combined observed limit. The region with blue shading shows the parameter space preferred by one of the models proposed to explain the B physics anomalies [61].

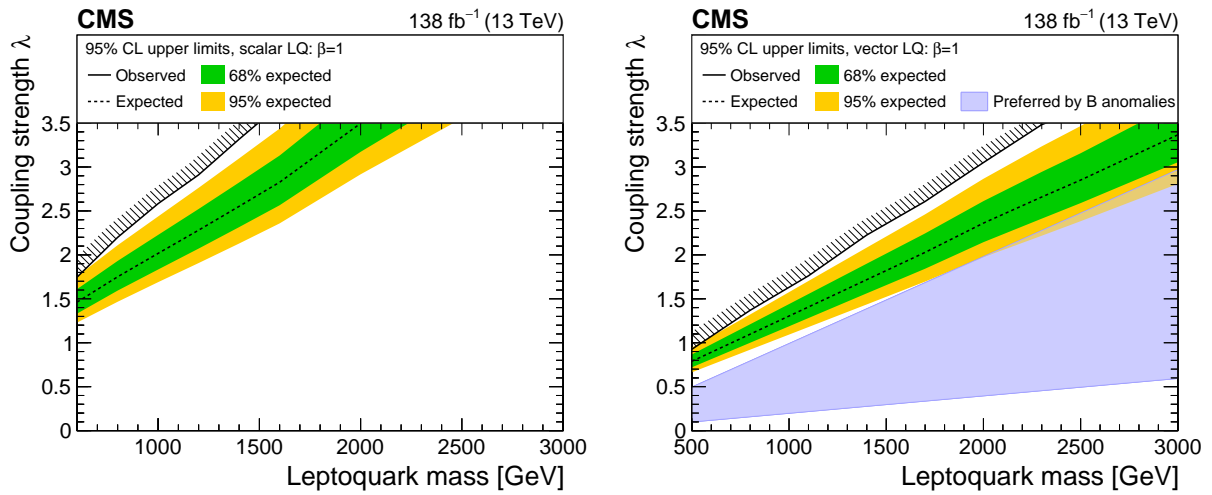


Figure 9: Observed and expected upper limit at the 95% CL on the coupling strength  $\lambda$  of a scalar (left) and vector LQ model (right) determined by considering only the nonresonant production of two  $\tau$  leptons through  $t$ -channel LQ exchange. Exclusive LQ couplings to  $b$  quarks and  $\tau$  leptons are assumed. The inner (green) band and the outer (yellow) band indicate the regions containing 68 and 95%, respectively, of the distribution of limits expected under the background-only hypothesis. The hatches indicate the excluded side of the parameter space with respect to the observed limit. The region with blue shading shows the parameter space preferred by one of the models proposed to explain the B physics anomalies [61].

## 9 Summary

A search has been presented for a third-generation leptoquark (LQ) decaying to a  $\tau$  lepton and a b quark. Events with  $\tau$  leptons and a varying number of jets originating from b quarks are considered, targeting the single and pair production of the LQs, as well as the nonresonant production of two  $\tau$  leptons through  $t$ -channel LQ exchange. The search uses proton-proton collision data at a center-of-mass energy of 13 TeV recorded with the CMS detector and corresponding to an integrated luminosity of  $138 \text{ fb}^{-1}$ . Upper limits are set on third-generation scalar and vector LQ production cross sections as a function of LQ mass, and results are compared with theoretical predictions to obtain lower limits on the LQ mass. At 95% confidence level, third-generation LQs decaying to a  $\tau$  lepton and a b quark with unit coupling ( $\lambda = 1$ ) are excluded for masses below 1.22 TeV for a scalar model, and below 1.50 (1.82) TeV for a vector model with a coupling parameter  $\kappa = 0(1)$ . For  $\lambda = 2.5$  the lower limits are 1.31 TeV for a scalar model, and 1.73 (1.88) TeV for a vector model with  $\kappa = 0(1)$ . The study of nonresonant  $\tau\tau$  production through  $t$ -channel LQ exchange allows lower limits on the LQ mass of up to 2.3 TeV to be obtained. Upper limits are also set on the coupling strengths of scalar and vector LQs as functions of their mass.

The observed data are found to agree with the standard model expectation within 2 standard deviations below a coupling strength of  $\lambda = 1.5$ . For a benchmark LQ model with a mass of 2 TeV and a coupling strength of 2.5, the data show an excess with a local significance of 2.8 standard deviations above the standard model expectation. Consequently, the observed upper limits on the LQ production cross section are about three times larger than expected for this benchmark. The present excess is driven by events with at least one highly energetic jet but no b-tagged jets, indicating the need for future similar analyses to consider alternative signal models.

## Acknowledgments

We congratulate our colleagues in the CERN accelerator departments for the excellent performance of the LHC and thank the technical and administrative staffs at CERN and at other CMS institutes for their contributions to the success of the CMS effort. In addition, we gratefully acknowledge the computing centers and personnel of the Worldwide LHC Computing Grid and other centers for delivering so effectively the computing infrastructure essential to our analyses. Finally, we acknowledge the enduring support for the construction and operation of the LHC, the CMS detector, and the supporting computing infrastructure provided by the following funding agencies: SC (Armenia), BMBWF and FWF (Austria); FNRS and FWO (Belgium); CNPq, CAPES, FAPERJ, FAPERGS, and FAPESP (Brazil); MES and BNSF (Bulgaria); CERN; CAS, MoST, and NSFC (China); MINCIENCIAS (Colombia); MSES and CSF (Croatia); RIF (Cyprus); SENESCYT (Ecuador); MoER, ERC PUT and ERDF (Estonia); Academy of Finland, MEC, and HIP (Finland); CEA and CNRS/IN2P3 (France); BMBF, DFG, and HGF (Germany); GSRI (Greece); NKFIH (Hungary); DAE and DST (India); IPM (Iran); SFI (Ireland); INFN (Italy); MSIP and NRF (Republic of Korea); MES (Latvia); LAS (Lithuania); MOE and UM (Malaysia); BUAP, CINVESTAV, CONACYT, LNS, SEP, and UASLP-FAI (Mexico); MOS (Montenegro); MBIE (New Zealand); PAEC (Pakistan); MES and NSC (Poland); FCT (Portugal); MESTD (Serbia); MCIN/AEI and PCTI (Spain); MOSTR (Sri Lanka); Swiss Funding Agencies (Switzerland); MST (Taipei); MHESI and NSTDA (Thailand); TUBITAK and TENMAK (Turkey); NASU (Ukraine); STFC (United Kingdom); DOE and NSF (USA).

Individuals have received support from the Marie-Curie program and the European Research



Council and Horizon 2020 Grant, contract Nos. 675440, 724704, 752730, 758316, 765710, 824093, and COST Action CA16108 (European Union); the Leventis Foundation; the Alfred P. Sloan Foundation; the Alexander von Humboldt Foundation; the Science Committee, project no. 22rl-037 (Armenia); the Belgian Federal Science Policy Office; the Fonds pour la Formation à la Recherche dans l'Industrie et dans l'Agriculture (FRIA-Belgium); the Agentschap voor Innovatie door Wetenschap en Technologie (IWT-Belgium); the F.R.S.-FNRS and FWO (Belgium) under the "Excellence of Science – EOS" – be.h project n. 30820817; the Beijing Municipal Science & Technology Commission, No. Z191100007219010 and Fundamental Research Funds for the Central Universities (China); the Ministry of Education, Youth and Sports (MEYS) of the Czech Republic; the Shota Rustaveli National Science Foundation, grant FR-22-985 (Georgia); the Deutsche Forschungsgemeinschaft (DFG), under Germany's Excellence Strategy – EXC 2121 "Quantum Universe" – 390833306, and under project number 400140256 - GRK2497; the Hellenic Foundation for Research and Innovation (HFRI), Project Number 2288 (Greece); the Hungarian Academy of Sciences, the New National Excellence Program - ÚNKP, the NKFIH research grants K 124845, K 124850, K 128713, K 128786, K 129058, K 131991, K 133046, K 138136, K 143460, K 143477, 2020-2.2.1-ED-2021-00181, and TKP2021-NKTA-64 (Hungary); the Council of Science and Industrial Research, India; the Latvian Council of Science; the Ministry of Education and Science, project no. 2022/WK/14, and the National Science Center, contracts Opus 2021/41/B/ST2/01369 and 2021/43/B/ST2/01552 (Poland); the Fundação para a Ciência e a Tecnologia, grant CEECIND/01334/2018 (Portugal); the National Priorities Research Program by Qatar National Research Fund; MCIN/AEI/10.13039/501100011033, ERDF "a way of making Europe", and the Programa Estatal de Fomento de la Investigación Científica y Técnica de Excelencia María de Maeztu, grant MDM-2017-0765 and Programa Severo Ochoa del Principado de Asturias (Spain); the Chulalongkorn Academic into Its 2nd Century Project Advancement Project, and the National Science, Research and Innovation Fund via the Program Management Unit for Human Resources & Institutional Development, Research and Innovation, grant B05F650021 (Thailand); the Kavli Foundation; the Nvidia Corporation; the SuperMicro Corporation; the Welch Foundation, contract C-1845; and the Weston Havens Foundation (USA).

## References

- [1] ATLAS Collaboration, "Observation of a new particle in the search for the standard model Higgs boson with the ATLAS detector at the LHC", *Phys. Lett. B* **716** (2012) 1, doi:10.1016/j.physletb.2012.08.020, arXiv:1207.7214.
- [2] CMS Collaboration, "Observation of a new boson at a mass of 125 GeV with the CMS experiment at the LHC", *Phys. Lett. B* **716** (2012) 30, doi:10.1016/j.physletb.2012.08.021, arXiv:1207.7235.
- [3] CMS Collaboration, "Observation of a new boson with mass near 125 GeV in pp collisions at  $\sqrt{s} = 7$  and 8 TeV", *JHEP* **06** (2013) 081, doi:10.1007/JHEP06(2013)081, arXiv:1303.4571.
- [4] BaBar Collaboration, "Evidence for an excess of  $\bar{B} \rightarrow D^{(*)} \tau^- \bar{\nu}_\tau$  decays", *Phys. Rev. Lett.* **109** (2012) 101802, doi:10.1103/PhysRevLett.109.101802, arXiv:1205.5442.
- [5] BaBar Collaboration, "Measurement of an excess of  $\bar{B} \rightarrow D^{(*)} \tau^- \bar{\nu}_\tau$  decays and implications for charged Higgs bosons", *Phys. Rev. D* **88** (2013) 072012, doi:10.1103/PhysRevD.88.072012, arXiv:1303.0571.

- [6] Belle Collaboration, “Observation of  $B^0 \rightarrow D^{*-} \tau^+ \nu_\tau$  decay at Belle”, *Phys. Rev. Lett.* **99** (2007) 191807, doi:10.1103/PhysRevLett.99.191807, arXiv:0706.4429.
- [7] Belle Collaboration, “Observation of  $B^+ \rightarrow \bar{D}^{*0} \tau^+ \nu_\tau$  and evidence for  $B^+ \rightarrow \bar{D}^0 \tau^+ \nu_\tau$  at Belle”, *Phys. Rev. D* **82** (2010) 072005, doi:10.1103/PhysRevD.82.072005, arXiv:1005.2302.
- [8] Belle Collaboration, “Measurement of the branching ratio of  $\bar{B} \rightarrow D^{(*)} \tau^- \bar{\nu}_\tau$  relative to  $\bar{B} \rightarrow D^{(*)} \ell^- \bar{\nu}_\ell$  decays with hadronic tagging at Belle”, *Phys. Rev. D* **92** (2015) 072014, doi:10.1103/PhysRevD.92.072014, arXiv:1507.03233.
- [9] Belle Collaboration, “Measurement of the branching ratio of  $\bar{B}^0 \rightarrow D^{*+} \tau^- \bar{\nu}_\tau$  relative to  $\bar{B}^0 \rightarrow D^{*+} \ell^- \bar{\nu}_\ell$  decays with a semileptonic tagging method”, *Phys. Rev. D* **94** (2016) 072007, doi:10.1103/PhysRevD.94.072007, arXiv:1607.07923.
- [10] Belle Collaboration, “Measurement of the  $\tau$  lepton polarization and  $R(D^*)$  in the decay  $\bar{B} \rightarrow D^* \tau^- \bar{\nu}_\tau$ ”, *Phys. Rev. Lett.* **118** (2017) 211801, doi:10.1103/PhysRevLett.118.211801, arXiv:1612.00529.
- [11] Belle Collaboration, “Measurement of the  $\tau$  lepton polarization and  $R(D^*)$  in the decay  $\bar{B} \rightarrow D^* \tau^- \bar{\nu}_\tau$  with one-prong hadronic  $\tau$  decays at Belle”, *Phys. Rev. D* **97** (2018) 012004, doi:10.1103/PhysRevD.97.012004, arXiv:1709.00129.
- [12] LHCb Collaboration, “Measurement of the ratio of branching fractions  $\mathcal{B}(\bar{B}^0 \rightarrow D^{*+} \tau^- \bar{\nu}_\tau) / \mathcal{B}(\bar{B}^0 \rightarrow D^{*+} \mu^- \bar{\nu}_\mu)$ ”, *Phys. Rev. Lett.* **115** (2015) 111803, doi:10.1103/PhysRevLett.115.111803, arXiv:1506.08614. [Erratum: doi:10.1103/PhysRevLett.115.159901].
- [13] LHCb Collaboration, “Measurement of the ratio of the  $B^0 \rightarrow D^{*-} \tau^+ \nu_\tau$  and  $B^0 \rightarrow D^{*-} \mu^+ \nu_\mu$  branching fractions using three-prong  $\tau$ -lepton decays”, *Phys. Rev. Lett.* **120** (2018) 171802, doi:10.1103/PhysRevLett.120.171802, arXiv:1708.08856.
- [14] LHCb Collaboration, “Test of lepton flavor universality by the measurement of the  $B^0 \rightarrow D^{*-} \tau^+ \nu_\tau$  branching fraction using three-prong  $\tau$  decays”, *Phys. Rev. D* **97** (2018) 072013, doi:10.1103/PhysRevD.97.072013, arXiv:1711.02505.
- [15] LHCb Collaboration, “Measurement of the ratios of branching fractions  $\mathcal{R}(D^*)$  and  $\mathcal{R}(D^0)$ ”, *Phys. Rev. Lett.* **131** (2023) 111802, doi:10.1103/PhysRevLett.131.111802, arXiv:2302.02886.
- [16] LHCb Collaboration, “Test of lepton flavor universality using  $B^0 \rightarrow D^{*-} \tau^+ \nu_\tau$  decays with hadronic  $\tau$  channels”, *Phys. Rev. D* **108** (2023) 012018, doi:10.1103/PhysRevD.108.012018, arXiv:2305.01463.
- [17] HFLAV Collaboration, “Averages of b-hadron, c-hadron, and  $\tau$ -lepton properties as of 2021”, *Phys. Rev. D* **107** (2023) 052008, doi:10.1103/PhysRevD.107.052008, arXiv:2206.07501.
- [18] J. C. Pati and A. Salam, “Unified lepton-hadron symmetry and a gauge theory of the basic interactions”, *Phys. Rev. D* **8** (1973) 1240, doi:10.1103/PhysRevD.8.1240.
- [19] H. Georgi and S. L. Glashow, “Unity of all elementary particle forces”, *Phys. Rev. Lett.* **32** (1974) 438, doi:10.1103/PhysRevLett.32.438.

- [20] J. C. Pati and A. Salam, "Lepton number as the fourth color", *Phys. Rev. D* **10** (1974) 275, doi:10.1103/PhysRevD.10.275. [Erratum: doi:10.1103/PhysRevD.11.703.2].
- [21] H. Fritzsch and P. Minkowski, "Unified interactions of leptons and hadrons", *Annals Phys.* **93** (1975) 193, doi:10.1016/0003-4916(75)90211-0.
- [22] G. Senjanovic and A. Sokorac, "Light leptoquarks in SO(10)", *Z. Phys. C* **20** (1983) 255, doi:10.1007/BF01574858.
- [23] P. H. Frampton and B.-H. Lee, "SU(15) grand unification", *Phys. Rev. Lett.* **64** (1990) 619, doi:10.1103/PhysRevLett.64.619.
- [24] P. H. Frampton and T. W. Kephart, "Higgs sector and proton decay in SU(15) grand unification", *Phys. Rev. D* **42** (1990) 3892, doi:10.1103/PhysRevD.42.3892.
- [25] H. Murayama and T. Yanagida, "A viable SU(5) GUT with light leptoquark bosons", *Mod. Phys. Lett. A* **7** (1992) 147, doi:10.1142/S0217732392000070.
- [26] S. Dimopoulos and L. Susskind, "Mass without scalars", *Nucl. Phys. B* **155** (1979) 237, doi:10.1016/0550-3213(79)90364-X.
- [27] S. Dimopoulos, "Technicolored signatures", *Nucl. Phys. B* **168** (1980) 69, doi:10.1016/0550-3213(80)90277-1.
- [28] E. Farhi and L. Susskind, "Technicolor", *Phys. Rept.* **74** (1981) 277, doi:10.1016/0370-1573(81)90173-3.
- [29] L. F. Abbott and E. Farhi, "Are the weak interactions strong?", *Phys. Lett. B* **101** (1981) 69, doi:10.1016/0370-2693(81)90492-5.
- [30] B. Schrempp and F. Schrempp, "Light leptoquarks", *Phys. Lett. B* **153** (1985) 101, doi:10.1016/0370-2693(85)91450-9.
- [31] J. Wudka, "Composite leptoquarks", *Phys. Lett. B* **167** (1986) 337, doi:10.1016/0370-2693(86)90356-4.
- [32] M. Tanaka and R. Watanabe, "New physics in the weak interaction of  $\bar{B} \rightarrow D^{(*)}\tau\bar{\nu}$ ", *Phys. Rev. D* **87** (2013) 034028, doi:10.1103/PhysRevD.87.034028, arXiv:1212.1878.
- [33] Y. Sakaki, M. Tanaka, A. Tayduganov, and R. Watanabe, "Testing leptoquark models in  $\bar{B} \rightarrow D^{(*)}\tau\bar{\nu}$ ", *Phys. Rev. D* **88** (2013) 094012, doi:10.1103/PhysRevD.88.094012, arXiv:1309.0301.
- [34] I. Doršner, S. Fajfer, N. Košnik, and I. Nišandžić, "Minimally flavored colored scalar in  $\bar{B} \rightarrow D^{(*)}\tau\bar{\nu}$  and the mass matrices constraints", *JHEP* **11** (2013) 084, doi:10.1007/JHEP11(2013)084, arXiv:1306.6493.
- [35] B. Gripaios, M. Nardecchia, and S. A. Renner, "Composite leptoquarks and anomalies in  $B$ -meson decays", *JHEP* **05** (2015) 006, doi:10.1007/JHEP05(2015)006, arXiv:1412.1791.
- [36] R. Alonso, B. Grinstein, and J. Martin Camalich, "Lepton universality violation and lepton flavor conservation in  $B$ -meson decays", *JHEP* **10** (2015) 184, doi:10.1007/JHEP10(2015)184, arXiv:1505.05164.

- [37] L. Calibbi, A. Crivellin, and T. Ota, “Effective field theory approach to  $b \rightarrow s\ell\ell^{(\prime)}$ ,  $B \rightarrow K^{(*)}\nu\bar{\nu}$  and  $B \rightarrow D^{(*)}\tau\nu$  with third generation couplings”, *Phys. Rev. Lett.* **115** (2015) 181801, doi:10.1103/PhysRevLett.115.181801, arXiv:1506.02661.
- [38] M. Bauer and M. Neubert, “Minimal leptoquark explanation for the  $R_{D^{(*)}}$ ,  $R_K$ , and  $(g-2)_\mu$  anomalies”, *Phys. Rev. Lett.* **116** (2016) 141802, doi:10.1103/PhysRevLett.116.141802, arXiv:1511.01900.
- [39] R. Barbieri, G. Isidori, A. Pattori, and F. Senia, “Anomalies in  $B$ -decays and  $U(2)$  flavour symmetry”, *Eur. Phys. J. C* **76** (2016) 67, doi:10.1140/epjc/s10052-016-3905-3, arXiv:1512.01560.
- [40] I. Doršner et al., “Physics of leptoquarks in precision experiments and at particle colliders”, *Phys. Rept.* **641** (2016) 1, doi:10.1016/j.physrep.2016.06.001, arXiv:1603.04993.
- [41] B. Dumont, K. Nishiwaki, and R. Watanabe, “LHC constraints and prospects for  $S_1$  scalar leptoquark explaining the  $\bar{B} \rightarrow D^{(*)}\tau\bar{\nu}$  anomaly”, *Phys. Rev. D* **94** (2016) 034001, doi:10.1103/PhysRevD.94.034001, arXiv:1603.05248.
- [42] E. Coluccio Leskow, G. D’Ambrosio, A. Crivellin, and D. Müller, “ $(g-2)_\mu$ , lepton flavor violation, and  $Z$  decays with leptoquarks: correlations and future prospects”, *Phys. Rev. D* **95** (2017) 055018, doi:10.1103/PhysRevD.95.055018, arXiv:1612.06858.
- [43] D. Bečirević and O. Sumensari, “A leptoquark model to accommodate  $R_K^{\text{exp}} < R_K^{\text{SM}}$  and  $R_{K^*}^{\text{exp}} < R_{K^*}^{\text{SM}}$ ”, *JHEP* **08** (2017) 104, doi:10.1007/JHEP08(2017)104, arXiv:1704.05835.
- [44] A. Crivellin, D. Müller, and T. Ota, “Simultaneous explanation of  $R(D^{(*)})$  and  $b \rightarrow s\mu^+\mu^-$ : the last scalar leptoquarks standing”, *JHEP* **09** (2017) 040, doi:10.1007/JHEP09(2017)040, arXiv:1703.09226.
- [45] D. Buttazzo, A. Greljo, G. Isidori, and D. Marzocca, “B-physics anomalies: a guide to combined explanations”, *JHEP* **11** (2017) 044, doi:10.1007/JHEP11(2017)044, arXiv:1706.07808.
- [46] G. Hiller and I. Nišandžić, “ $R_K$  and  $R_{K^*}$  beyond the standard model”, *Phys. Rev. D* **96** (2017) 035003, doi:10.1103/PhysRevD.96.035003, arXiv:1704.05444.
- [47] I. Doršner, S. Fajfer, D. A. Faroughy, and N. Košnik, “The role of the  $S_3$  GUT leptoquark in flavor universality and collider searches”, *JHEP* **10** (2017) 188, doi:10.1007/JHEP10(2017)188, arXiv:1706.07779.
- [48] L. Di Luzio, A. Greljo, and M. Nardecchia, “Gauge leptoquark as the origin of B-physics anomalies”, *Phys. Rev. D* **96** (2017) 115011, doi:10.1103/PhysRevD.96.115011, arXiv:1708.08450.
- [49] L. Calibbi, A. Crivellin, and T. Li, “Model of vector leptoquarks in view of the B-physics anomalies”, *Phys. Rev. D* **98** (2018) 115002, doi:10.1103/PhysRevD.98.115002, arXiv:1709.00692.
- [50] M. Bordone, C. Cornella, J. Fuentes-Martín, and G. Isidori, “A three-site gauge model for flavor hierarchies and flavor anomalies”, *Phys. Lett. B* **779** (2018) 317, doi:10.1016/j.physletb.2018.02.011, arXiv:1712.01368.

- [51] G. Hiller, D. Loose, and I. Nišandžić, “Flavorful leptoquarks at hadron colliders”, *Phys. Rev. D* **97** (2018) 075004, doi:10.1103/PhysRevD.97.075004, arXiv:1801.09399.
- [52] D. Bečirević et al., “Scalar leptoquarks from grand unified theories to accommodate the  $B$ -physics anomalies”, *Phys. Rev. D* **98** (2018) 055003, doi:10.1103/PhysRevD.98.055003, arXiv:1806.05689.
- [53] L. Di Luzio et al., “Maximal flavour violation: a Cabibbo mechanism for leptoquarks”, *JHEP* **11** (2018) 081, doi:10.1007/JHEP11(2018)081, arXiv:1808.00942.
- [54] R. Barbieri and A. Tesi, “ $B$ -decay anomalies in Pati-Salam  $SU(4)$ ”, *Eur. Phys. J. C* **78** (2018) 193, doi:10.1140/epjc/s10052-018-5680-9, arXiv:1712.06844.
- [55] D. Marzocca, “Addressing the  $B$ -physics anomalies in a fundamental composite Higgs model”, *JHEP* **07** (2018) 121, doi:10.1007/JHEP07(2018)121, arXiv:1803.10972.
- [56] A. Angelescu, D. Bečirević, D. A. Faroughy, and O. Sumensari, “Closing the window on single leptoquark solutions to the  $B$ -physics anomalies”, *JHEP* **10** (2018) 183, doi:10.1007/JHEP10(2018)183, arXiv:1808.08179.
- [57] J. Kumar, D. London, and R. Watanabe, “Combined explanations of the  $b \rightarrow s\mu^+\mu^-$  and  $b \rightarrow c\tau^-\bar{\nu}$  anomalies: a general model analysis”, *Phys. Rev. D* **99** (2019) 015007, doi:10.1103/PhysRevD.99.015007, arXiv:1806.07403.
- [58] M. J. Baker, J. Fuentes-Martín, G. Isidori, and M. König, “High- $p_T$  signatures in vector-leptoquark models”, *Eur. Phys. J. C* **79** (2019) 334, doi:10.1140/epjc/s10052-019-6853-x, arXiv:1901.10480.
- [59] C. Cornella, J. Fuentes-Martín, and G. Isidori, “Revisiting the vector leptoquark explanation of the  $B$ -physics anomalies”, *JHEP* **07** (2019) 168, doi:10.1007/JHEP07(2019)168, arXiv:1903.11517.
- [60] A. Angelescu et al., “Single leptoquark solutions to the  $B$ -physics anomalies”, *Phys. Rev. D* **104** (2021) 055017, doi:10.1103/PhysRevD.104.055017, arXiv:2103.12504.
- [61] C. Cornella et al., “Reading the footprints of the  $B$ -meson flavor anomalies”, *JHEP* **08** (2021) 050, doi:10.1007/JHEP08(2021)050, arXiv:2103.16558.
- [62] G. Isidori, D. Lancierini, P. Owen, and N. Serra, “On the significance of new physics in  $b \rightarrow s\ell^+\ell^-$  decays”, *Phys. Lett. B* **822** (2021) 136644, doi:10.1016/j.physletb.2021.136644, arXiv:2104.05631.
- [63] J. Aebischer et al., “Confronting the vector leptoquark hypothesis with new low- and high-energy data”, *Eur. Phys. J. C* **83** (2023) 153, doi:10.1140/epjc/s10052-023-11304-5, arXiv:2210.13422.
- [64] LHCb Collaboration, “Differential branching fractions and isospin asymmetries of  $B \rightarrow K^{(*)}\mu^+\mu^-$  decays”, *JHEP* **06** (2014) 133, doi:10.1007/JHEP06(2014)133, arXiv:1403.8044.
- [65] LHCb Collaboration, “Measurements of the  $S$ -wave fraction in  $B^0 \rightarrow K^+\pi^-\mu^+\mu^-$  decays and the  $B^0 \rightarrow K^*(892)^0\mu^+\mu^-$  differential branching fraction”, *JHEP* **11** (2016) 047, doi:10.1007/JHEP11(2016)047, arXiv:1606.04731. [Erratum: doi:10.1007/JHEP04(2017)142].

- [66] LHCb Collaboration, “Angular analysis and differential branching fraction of the decay  $B_s^0 \rightarrow \phi \mu^+ \mu^-$ ”, *JHEP* **09** (2015) 179, doi:10.1007/JHEP09(2015)179, arXiv:1506.08777.
- [67] LHCb Collaboration, “Angular analysis of the  $B^0 \rightarrow K^{*0} \mu^+ \mu^-$  decay using  $3 \text{ fb}^{-1}$  of integrated luminosity”, *JHEP* **02** (2016) 104, doi:10.1007/JHEP02(2016)104, arXiv:1512.04442.
- [68] LHCb Collaboration, “Measurement of  $CP$ -averaged observables in the  $B^0 \rightarrow K^{*0} \mu^+ \mu^-$  decay”, *Phys. Rev. Lett.* **125** (2020) 011802, doi:10.1103/PhysRevLett.125.011802, arXiv:2003.04831.
- [69] LHCb Collaboration, “Angular analysis of the  $B^+ \rightarrow K^{*+} \mu^+ \mu^-$  decay”, *Phys. Rev. Lett.* **126** (2021) 161802, doi:10.1103/PhysRevLett.126.161802, arXiv:2012.13241.
- [70] Belle Collaboration, “Lepton-flavor-dependent angular analysis of  $B \rightarrow K^* \ell^+ \ell^-$ ”, *Phys. Rev. Lett.* **118** (2017) 111801, doi:10.1103/PhysRevLett.118.111801, arXiv:1612.05014.
- [71] W. Buchmuller, R. Ruckl, and D. Wyler, “Leptoquarks in lepton-quark collisions”, *Phys. Lett. B* **191** (1987) 442, doi:10.1016/0370-2693(87)90637-X. [Erratum: doi:10.1016/S0370-2693(99)00014-3].
- [72] J. Blümlein, E. Boos, and A. Kryukov, “Leptoquark pair production in hadronic interactions”, *Z. Phys. C* **76** (1997) 137, doi:10.1007/s002880050538, arXiv:hep-ph/9610408.
- [73] I. Doršner and A. Greljo, “Leptoquark toolbox for precision collider studies”, *JHEP* **05** (2018) 126, doi:10.1007/JHEP05(2018)126, arXiv:1801.07641.
- [74] D. A. Faroughy, A. Greljo, and J. F. Kamenik, “Confronting lepton flavor universality violation in B decays with high- $p_T$  tau lepton searches at LHC”, *Phys. Lett. B* **764** (2017) 126, doi:10.1016/j.physletb.2016.11.011, arXiv:1609.07138.
- [75] M. Schmaltz and Y.-M. Zhong, “The leptoquark hunter’s guide: large coupling”, *JHEP* **01** (2019) 132, doi:10.1007/JHEP01(2019)132, arXiv:1810.10017.
- [76] ATLAS Collaboration, “Search for pair production of third-generation leptoquarks decaying into a bottom quark and a  $\tau$ -lepton with the ATLAS detector”, *Eur. Phys. J. C* **83** (2023) 1075, doi:10.1140/epjc/s10052-023-12104-7, arXiv:2303.01294.
- [77] ATLAS Collaboration, “Search for leptoquarks decaying into the  $b\tau$  final state in  $pp$  collisions at  $\sqrt{s} = 13 \text{ TeV}$  with the ATLAS detector”, *JHEP* **10** (2023) 001, doi:10.1007/JHEP10(2023)001, arXiv:2305.15962.
- [78] CMS Collaboration, “Search for a singly produced third-generation scalar leptoquark decaying to a  $\tau$  lepton and a bottom quark in proton-proton collisions at  $\sqrt{s} = 13 \text{ TeV}$ ”, *JHEP* **07** (2018) 115, doi:10.1007/JHEP07(2018)115, arXiv:1806.03472.
- [79] CMS Collaboration, “Searches for physics beyond the standard model with the  $M_{T2}$  variable in hadronic final states with and without disappearing tracks in proton-proton collisions at  $\sqrt{s} = 13 \text{ TeV}$ ”, *Eur. Phys. J. C* **80** (2020) 3, doi:10.1140/epjc/s10052-019-7493-x, arXiv:1909.03460.

- [80] CMS Collaboration, “Search for singly and pair-produced leptoquarks coupling to third-generation fermions in proton-proton collisions at  $\sqrt{s} = 13$  TeV”, *Phys. Lett. B* **819** (2021) 136446, doi:10.1016/j.physletb.2021.136446, arXiv:2012.04178.
- [81] ATLAS Collaboration, “Search for pair production of third-generation scalar leptoquarks decaying into a top quark and a  $\tau$ -lepton in  $pp$  collisions at  $\sqrt{s} = 13$  TeV with the ATLAS detector”, *JHEP* **06** (2021) 179, doi:10.1007/JHEP06(2021)179, arXiv:2101.11582.
- [82] ATLAS Collaboration, “Search for new phenomena in  $pp$  collisions in final states with tau leptons, b-jets, and missing transverse momentum with the ATLAS detector”, *Phys. Rev. D* **104** (2021) 112005, doi:10.1103/PhysRevD.104.112005, arXiv:2108.07665.
- [83] “HEPData record for this analysis”, 2023. doi:10.17182/hepdata.141707.
- [84] CMS Collaboration, “The CMS experiment at the CERN LHC”, *JINST* **3** (2008) S08004, doi:10.1088/1748-0221/3/08/S08004.
- [85] CMS Collaboration, “The CMS trigger system”, *JINST* **12** (2017) P01020, doi:10.1088/1748-0221/12/01/P01020, arXiv:1609.02366.
- [86] CMS Collaboration, “Performance of the CMS level-1 trigger in proton-proton collisions at  $\sqrt{s} = 13$  TeV”, *JINST* **15** (2020) P10017, doi:10.1088/1748-0221/15/10/P10017, arXiv:2006.10165.
- [87] J. Alwall et al., “The automated computation of tree-level and next-to-leading order differential cross sections, and their matching to parton shower simulations”, *JHEP* **07** (2014) 079, doi:10.1007/JHEP07(2014)079, arXiv:1405.0301.
- [88] J. Alwall et al., “Comparative study of various algorithms for the merging of parton showers and matrix elements in hadronic collisions”, *Eur. Phys. J. C* **53** (2008) 473, doi:10.1140/epjc/s10052-007-0490-5, arXiv:0706.2569.
- [89] T. Sjöstrand et al., “An introduction to PYTHIA 8.2”, *Comput. Phys. Commun.* **191** (2015) 159, doi:10.1016/j.cpc.2015.01.024, arXiv:1410.3012.
- [90] J. M. Campbell and R. K. Ellis, “An update on vector boson pair production at hadron colliders”, *Phys. Rev. D* **60** (1999) 113006, doi:10.1103/PhysRevD.60.113006, arXiv:hep-ph/9905386.
- [91] J. M. Campbell, R. K. Ellis, and C. Williams, “Vector boson pair production at the LHC”, *JHEP* **07** (2011) 18, doi:10.1007/JHEP07(2011)018, arXiv:1105.0020.
- [92] J. M. Campbell, R. K. Ellis, and W. T. Giele, “A multi-threaded version of MCFM”, *Eur. Phys. J. C* **75** (2015) 246, doi:10.1140/epjc/s10052-015-3461-2, arXiv:1503.06182.
- [93] P. Nason, “A new method for combining NLO QCD with shower Monte Carlo algorithms”, *JHEP* **11** (2004) 040, doi:10.1088/1126-6708/2004/11/040, arXiv:hep-ph/0409146.
- [94] S. Frixione, P. Nason, and C. Oleari, “Matching NLO QCD computations with parton shower simulations: the POWHEG method”, *JHEP* **11** (2007) 070, doi:10.1088/1126-6708/2007/11/070, arXiv:0709.2092.

- 
- [95] S. Alioli, P. Nason, C. Oleari, and E. Re, “A general framework for implementing NLO calculations in shower Monte Carlo programs: the POWHEG BOX”, *JHEP* **06** (2010) 043, doi:10.1007/JHEP06(2010)043, arXiv:1002.2581.
- [96] S. Frixione, P. Nason, and G. Ridolfi, “A positive-weight next-to-leading-order Monte Carlo for heavy flavour hadroproduction”, *JHEP* **09** (2007) 126, doi:10.1088/1126-6708/2007/09/126, arXiv:0707.3088.
- [97] J. M. Campbell, R. K. Ellis, P. Nason, and E. Re, “Top-pair production and decay at NLO matched with parton showers”, *JHEP* **04** (2015) 114, doi:10.1007/JHEP04(2015)114, arXiv:1412.1828.
- [98] S. Alioli, P. Nason, C. Oleari, and E. Re, “NLO single-top production matched with shower in POWHEG:  $s$ - and  $t$ -channel contributions”, *JHEP* **09** (2009) 111, doi:10.1088/1126-6708/2009/09/111, arXiv:0907.4076. [Erratum: doi:10.1007/JHEP02(2010)011].
- [99] E. Re, “Single-top  $Wt$ -channel production matched with parton showers using the POWHEG method”, *Eur. Phys. J. C* **71** (2011) 1547, doi:10.1140/epjc/s10052-011-1547-z, arXiv:1009.2450.
- [100] Y. Li and F. Petriello, “Combining QCD and electroweak corrections to production in FEWZ”, *Phys. Rev. D* **86** (2012) 094034, doi:10.1103/PhysRevD.86.094034, arXiv:1208.5967.
- [101] M. Czakon and A. Mitov, “Top++: a program for the calculation of the top-pair cross-section at hadron colliders”, *Comput. Phys. Commun.* **185** (2014) 2930, doi:10.1016/j.cpc.2014.06.021, arXiv:1112.5675.
- [102] P. Kant et al., “HATHOR for single top-quark production: updated predictions and uncertainty estimates for single top-quark production in hadronic collisions”, *Comput. Phys. Commun.* **191** (2015) 74, doi:10.1016/j.cpc.2015.02.001, arXiv:1406.4403.
- [103] F. Maltoni and T. Stelzer, “MadEvent: automatic event generation with MadGraph”, *JHEP* **02** (2003) 027, doi:10.1088/1126-6708/2003/02/027, arXiv:hep-ph/0208156.
- [104] M. Krämer, T. Plehn, M. Spira, and P. M. Zerwas, “Pair production of scalar leptoquarks at the Tevatron”, *Phys. Rev. Lett.* **79** (1997) 341, doi:10.1103/PhysRevLett.79.341, arXiv:hep-ph/9704322.
- [105] M. Krämer, T. Plehn, M. Spira, and P. M. Zerwas, “Pair production of scalar leptoquarks at the CERN LHC”, *Phys. Rev. D* **71** (2005) 057503, doi:10.1103/PhysRevD.71.057503, arXiv:hep-ph/0411038.
- [106] C. Borschensky, B. Fuks, A. Kulesza, and D. Schwartländer, “Scalar leptoquark pair production at hadron colliders”, *Phys. Rev. D* **101** (2020) 115017, doi:10.1103/PhysRevD.101.115017, arXiv:2002.08971.
- [107] CMS Collaboration, “Event generator tunes obtained from underlying event and multiparton scattering measurements”, *Eur. Phys. J. C* **76** (2016) 155, doi:10.1140/epjc/s10052-016-3988-x, arXiv:1512.00815.



- [108] CMS Collaboration, “Extraction and validation of a new set of CMS PYTHIA8 tunes from underlying-event measurements”, *Eur. Phys. J. C* **80** (2020) 4, doi:10.1140/epjc/s10052-019-7499-4, arXiv:1903.12179.
- [109] CMS Collaboration, “Investigations of the impact of the parton shower tuning in Pythia 8 in the modelling of  $t\bar{t}$  at  $\sqrt{s} = 8$  and 13 TeV”, CMS Physics Analysis Summary CMS-PAS-TOP-16-021, 2016.
- [110] NNPDF Collaboration, “Parton distributions for the LHC Run II”, *JHEP* **04** (2015) 040, doi:10.1007/JHEP04(2015)040, arXiv:1410.8849.
- [111] NNPDF Collaboration, “Parton distributions from high-precision collider data”, *Eur. Phys. J. C* **77** (2017) 663, doi:10.1140/epjc/s10052-017-5199-5, arXiv:1706.00428.
- [112] GEANT4 Collaboration, “GEANT4—a simulation toolkit”, *Nucl. Instrum. Meth. A* **506** (2003) 250, doi:10.1016/S0168-9002(03)01368-8.
- [113] CMS Collaboration, “Particle-flow reconstruction and global event description with the CMS detector”, *JINST* **12** (2017) P10003, doi:10.1088/1748-0221/12/10/P10003, arXiv:1706.04965.
- [114] CMS Collaboration, “Technical proposal for the Phase-II upgrade of the Compact Muon Solenoid”, CMS Technical Proposal CERN-LHCC-2015-010, CMS-TDR-15-02, 2015.
- [115] CMS Collaboration, “ECAL 2016 refined calibration and Run2 summary plots”, CMS Detector Performance Summary CMS-DP-2020-021, 2020.
- [116] CMS Collaboration, “Electron and photon reconstruction and identification with the CMS experiment at the CERN LHC”, *JINST* **16** (2021) P05014, doi:10.1088/1748-0221/16/05/P05014, arXiv:2012.06888.
- [117] A. Hoecker et al., “TMVA - Toolkit for multivariate data analysis”, 2007. arXiv:physics/0703039.
- [118] CMS Collaboration, “Performance of the CMS muon detector and muon reconstruction with proton-proton collisions at  $\sqrt{s} = 13$  TeV”, *JINST* **13** (2018) P06015, doi:10.1088/1748-0221/13/06/P06015, arXiv:1804.04528.
- [119] M. Cacciari, G. P. Salam, and G. Soyez, “The anti- $k_T$  jet clustering algorithm”, *JHEP* **04** (2008) 063, doi:10.1088/1126-6708/2008/04/063, arXiv:0802.1189.
- [120] M. Cacciari, G. P. Salam, and G. Soyez, “FastJet user manual”, *Eur. Phys. J. C* **72** (2012) 1896, doi:10.1140/epjc/s10052-012-1896-2, arXiv:1111.6097.
- [121] CMS Collaboration, “Jet energy scale and resolution in the CMS experiment in pp collisions at 8 TeV”, *JINST* **12** (2017) P02014, doi:10.1088/1748-0221/12/02/P02014, arXiv:1607.03663.
- [122] D. Guest et al., “Jet flavor classification in high-energy physics with deep neural networks”, *Phys. Rev. D* **94** (2016) 112002, doi:10.1103/PhysRevD.94.112002, arXiv:1607.08633.
- [123] CMS Collaboration, “Identification of heavy-flavour jets with the CMS detector in pp collisions at 13 TeV”, *JINST* **13** (2018) P05011, doi:10.1088/1748-0221/13/05/P05011, arXiv:1712.07158.

- [124] CMS Collaboration, “Identification of b-quark jets with the CMS experiment”, *JINST* **8** (2013) P04013, doi:10.1088/1748-0221/8/04/P04013, arXiv:1211.4462.
- [125] CMS Collaboration, “Performance of reconstruction and identification of  $\tau$  leptons decaying to hadrons and  $\nu_\tau$  in pp collisions at  $\sqrt{s} = 13$  TeV”, *JINST* **13** (2018) P10005, doi:10.1088/1748-0221/13/10/P10005, arXiv:1809.02816.
- [126] CMS Collaboration, “Identification of hadronic tau lepton decays using a deep neural network”, *JINST* **17** (2022) P07023, doi:10.1088/1748-0221/17/07/p07023, arXiv:2201.08458.
- [127] CMS Collaboration, “Performance of missing transverse momentum reconstruction in proton-proton collisions at  $\sqrt{s} = 13$  TeV using the CMS detector”, *JINST* **14** (2019) P07004, doi:10.1088/1748-0221/14/07/P07004, arXiv:1903.06078.
- [128] B. L. Combridge and C. J. Maxwell, “Untangling large- $p_T$  hadronic reactions”, *Nucl. Phys. B* **239** (1984) 429, doi:10.1016/0550-3213(84)90257-8.
- [129] CMS Collaboration, “Search for additional neutral MSSM Higgs bosons in the  $\tau\tau$  final state in proton-proton collisions at  $\sqrt{s} = 13$  TeV”, *JHEP* **09** (2018) 007, doi:10.1007/JHEP09(2018)007, arXiv:1803.06553.
- [130] CMS Collaboration, “Measurement of the  $Z\gamma^* \rightarrow \tau\tau$  cross section in pp collisions at  $\sqrt{s} = 13$  TeV and validation of  $\tau$  lepton analysis techniques”, *Eur. Phys. J. C* **78** (2018) 708, doi:10.1140/epjc/s10052-018-6146-9, arXiv:1801.03535.
- [131] CMS Collaboration, “Precision luminosity measurement in proton-proton collisions at  $\sqrt{s} = 13$  TeV in 2015 and 2016 at CMS”, *Eur. Phys. J. C* **81** (2021) 800, doi:10.1140/epjc/s10052-021-09538-2, arXiv:2104.01927.
- [132] CMS Collaboration, “CMS luminosity measurement for the 2017 data-taking period at  $\sqrt{s} = 13$  TeV”, CMS Physics Analysis Summary CMS-PAS-LUM-17-004, 2018.
- [133] CMS Collaboration, “CMS luminosity measurement for the 2018 data-taking period at  $\sqrt{s} = 13$  TeV”, CMS Physics Analysis Summary CMS-PAS-LUM-18-002, 2019.
- [134] CMS Collaboration, “Observation of the Higgs boson decay to a pair of  $\tau$  leptons with the CMS detector”, *Phys. Lett. B* **779** (2018) 283, doi:10.1016/j.physletb.2018.02.004, arXiv:1708.00373.
- [135] CMS Collaboration, “Performance of reconstruction and identification of tau leptons in their decays to hadrons and tau neutrino in LHC Run-2”, CMS Physics Analysis Summary CMS-PAS-TAU-16-002, 2016.
- [136] CMS Collaboration, “Measurement of the inclusive W and Z production cross sections in pp collisions at  $\sqrt{s} = 7$  TeV”, *JHEP* **10** (2011) 132, doi:10.1007/JHEP10(2011)132, arXiv:1107.4789.
- [137] CMS Collaboration, “Determination of jet energy calibration and transverse momentum resolution in CMS”, *JINST* **6** (2011) P11002, doi:10.1088/1748-0221/6/11/P11002, arXiv:1107.4277.
- [138] CMS Collaboration, “Measurement of differential  $t\bar{t}$  production cross sections in the full kinematic range using lepton+jets events from proton-proton collisions at  $\sqrt{s} = 13$  TeV”, *Phys. Rev. D* **104** (2021) 092013, doi:10.1103/PhysRevD.104.092013, arXiv:2108.02803.

- [139] ATLAS Collaboration, “Measurements of differential cross-sections in top-quark pair events with a high transverse momentum top quark and limits on beyond the standard model contributions to top-quark pair production with the ATLAS detector at  $\sqrt{s} = 13$  TeV”, *JHEP* **06** (2022) 063, doi:10.1007/JHEP06(2022)063, arXiv:2202.12134.
- [140] ATLAS Collaboration, “Differential  $t\bar{t}$  cross-section measurements using boosted top quarks in the all-hadronic final state with  $139 \text{ fb}^{-1}$  of ATLAS data”, *JHEP* **04** (2023) 080, doi:10.1007/JHEP04(2023)080, arXiv:2205.02817.
- [141] CMS Collaboration, “Search for a heavy resonance decaying to a top quark and a W boson at  $\sqrt{s} = 13$  TeV in the fully hadronic final state”, *JHEP* **12** (2021) 106, doi:10.1007/JHEP12(2021)106, arXiv:2104.12853.
- [142] J. Butterworth et al., “PDF4LHC recommendations for LHC Run II”, *J. Phys. G* **43** (2016) 023001, doi:10.1088/0954-3899/43/2/023001, arXiv:1510.03865.
- [143] R. J. Barlow and C. Beeston, “Fitting using finite Monte Carlo samples”, *Comput. Phys. Commun.* **77** (1993) 219, doi:10.1016/0010-4655(93)90005-w.
- [144] J. S. Conway, “Incorporating nuisance parameters in likelihoods for multisource spectra”, in *PHYSTAT 2011*, p. 115. 2011. arXiv:1103.0354. doi:10.5170/CERN-2011-006.115.
- [145] ATLAS and CMS Collaborations, and LHC Higgs Combination Group, “Procedure for the LHC Higgs boson search combination in Summer 2011”, Technical Report CMS-NOTE-2011-005, ATL-PHYS-PUB-2011-11, 2011.
- [146] G. Cowan, K. Cranmer, E. Gross, and O. Vitells, “Asymptotic formulae for likelihood-based tests of new physics”, *Eur. Phys. J. C* **71** (2011) 1554, doi:10.1140/epjc/s10052-011-1554-0, arXiv:1007.1727. [Erratum: doi:10.1140/epjc/s10052-013-2501-z].
- [147] CMS Collaboration, “Searches for additional Higgs bosons and for vector leptoquarks in  $\tau\tau$  final states in proton-proton collisions at  $\sqrt{s} = 13$  TeV”, *JHEP* **07** (2023) 073, doi:10.1007/JHEP07(2023)073, arXiv:2208.02717.
- [148] T. Junk, “Confidence level computation for combining searches with small statistics”, *Nucl. Instrum. Meth. A* **434** (1999) 435, doi:10.1016/S0168-9002(99)00498-2, arXiv:hep-ex/9902006.
- [149] A. L. Read, “Presentation of search results: the  $CL_s$  technique”, *J. Phys. G* **28** (2002) 2693, doi:10.1088/0954-3899/28/10/313.





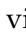
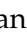




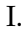









## A The CMS Collaboration




### Yerevan Physics Institute, Yerevan, Armenia

A. Hayrapetyan, A. Tumasyan<sup>1</sup> 

### Institut für Hochenergiephysik, Vienna, Austria

W. Adam , J.W. Andrejkovic, T. Bergauer , S. Chatterjee , K. Damanakis , M. Dragicevic , A. Escalante Del Valle , P.S. Hussain , M. Jeitler<sup>2</sup> , N. Krammer , D. Liko , I. Mikulec , J. Schieck<sup>2</sup> , R. Schöffbeck , D. Schwarz , M. Sonawane , S. Templ , W. Waltenberger , C.-E. Wulz<sup>2</sup> 















### Universiteit Antwerpen, Antwerpen, Belgium

M.R. Darwish<sup>3</sup> , T. Janssen , P. Van Mechelen 

### Vrije Universiteit Brussel, Brussel, Belgium

E.S. Bols , J. D'Hondt , S. Dansana , A. De Moor , M. Delcourt , H. El Faham , S. Lowette , I. Makarenko , D. Müller , A.R. Sahasransu , S. Tavernier , M. Tytgat<sup>4</sup> , S. Van Putte , D. Vannerom 

### Université Libre de Bruxelles, Bruxelles, Belgium

B. Clerbaux , G. De Lentdecker , L. Favart , D. Hohov , J. Jaramillo , A. Khalilzadeh, K. Lee , M. Mahdavihorrani , A. Malara , S. Paredes , L. Pétré , N. Postiau, L. Thomas , M. Vanden Bemden , C. Vander Velde , P. Vanlaer 






### Ghent University, Ghent, Belgium

M. De Coen , D. Dobur , Y. Hong , J. Knolle , L. Lambrecht , G. Mestdach, C. Rendón, A. Samalan, K. Skovpen , N. Van Den Bossche , L. Wezenbeek 


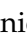





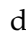










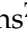
### Université Catholique de Louvain, Louvain-la-Neuve, Belgium

A. Benecke , G. Bruno , C. Caputo , C. Delaere , I.S. Donertas , A. Giammanco , K. Jaffel , Sa. Jain , V. Lemaitre, J. Lidrych , P. Mastrapasqua , K. Mondal , T.T. Tran , S. Wertz 

### Centro Brasileiro de Pesquisas Físicas, Rio de Janeiro, Brazil

G.A. Alves , E. Coelho , C. Hensel , T. Menezes De Oliveira, A. Moraes , P. Rebello Teles , M. Soeiro

### Universidade do Estado do Rio de Janeiro, Rio de Janeiro, Brazil

W.L. Aldá Júnior , M. Alves Gallo Pereira , M. Barroso Ferreira Filho , H. Brandao Malbouisson , W. Carvalho , J. Chinellato<sup>5</sup>, E.M. Da Costa , G.G. Da Silveira<sup>6</sup> , D. De Jesus Damiao , S. Fonseca De Souza , J. Martins<sup>7</sup> , C. Mora Herrera , K. Mota Amarilo , L. Mundim , H. Nogima , A. Santoro , S.M. Silva Do Amaral , A. Sznajder , M. Thiel , A. Vilela Pereira 

### Universidade Estadual Paulista, Universidade Federal do ABC, São Paulo, Brazil

C.A. Bernardes<sup>6</sup> , L. Calligaris , T.R. Fernandez Perez Tomei , E.M. Gregores , P.G. Mercadante , S.F. Novaes , B. Orzari , Sandra S. Padula 

### Institute for Nuclear Research and Nuclear Energy, Bulgarian Academy of Sciences, Sofia, Bulgaria

A. Aleksandrov , G. Antchev , R. Hadjiiska , P. Iaydjiev , M. Misheva , M. Shopova , G. Sultanov 





### University of Sofia, Sofia, Bulgaria

A. Dimitrov , T. Ivanov , L. Litov , B. Pavlov , P. Petkov , A. Petrov , E. Shumka 

**Instituto De Alta Investigación, Universidad de Tarapacá, Casilla 7 D, Arica, Chile**

S. Keshri , S. Thakur 




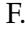


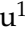
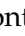




**Beihang University, Beijing, China**

T. Cheng , Q. Guo, T. Javaid , M. Mittal , L. Yuan 

**Department of Physics, Tsinghua University, Beijing, China**

G. Bauer<sup>8,9</sup>, Z. Hu , J. Liu, K. Yi<sup>8,10</sup> 

**Institute of High Energy Physics, Beijing, China**

G.M. Chen<sup>11</sup> , H.S. Chen<sup>11</sup> , M. Chen<sup>11</sup> , F. Iemmi , C.H. Jiang, A. Kapoor<sup>12</sup> , H. Liao , Z.-A. Liu<sup>13</sup> , F. Monti , M.A. Shahzad<sup>11</sup>, R. Sharma<sup>14</sup> , J.N. Song<sup>13</sup>, J. Tao , C. Wang<sup>11</sup>, J. Wang , Z. Wang<sup>11</sup>, H. Zhang 


**State Key Laboratory of Nuclear Physics and Technology, Peking University, Beijing, China**

A. Agapitos , Y. Ban , A. Levin , C. Li , Q. Li , Y. Mao, S.J. Qian , X. Sun , D. Wang , H. Yang, L. Zhang , C. Zhou 



**Sun Yat-Sen University, Guangzhou, China**

Z. You 

**University of Science and Technology of China, Hefei, China**

N. Lu 

**Institute of Modern Physics and Key Laboratory of Nuclear Physics and Ion-beam Application (MOE) - Fudan University, Shanghai, China**

X. Gao<sup>15</sup> , D. Leggat, H. Okawa , Y. Zhang 



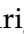

**Zhejiang University, Hangzhou, Zhejiang, China**

Z. Lin , C. Lu , M. Xiao 


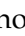

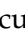
**Universidad de Los Andes, Bogota, Colombia**

C. Avila , D.A. Barbosa Trujillo, A. Cabrera , C. Florez , J. Fraga , J.A. Reyes Vega

**Universidad de Antioquia, Medellin, Colombia**

J. Mejia Guisao , F. Ramirez , M. Rodriguez , J.D. Ruiz Alvarez 

**University of Split, Faculty of Electrical Engineering, Mechanical Engineering and Naval Architecture, Split, Croatia**

D. Giljanovic , N. Godinovic , D. Lelas , A. Sculac 









**University of Split, Faculty of Science, Split, Croatia**

M. Kovac , T. Sculac 




**Institute Rudjer Boskovic, Zagreb, Croatia**

P. Bargassa , V. Brigljevic , B.K. Chitroda , D. Ferencek , S. Mishra , A. Starodumov<sup>16</sup> , T. Susa 

**University of Cyprus, Nicosia, Cyprus**




















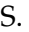
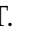








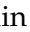



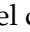
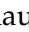




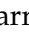


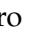
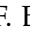
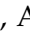


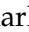

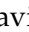


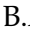





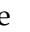










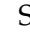




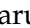
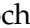
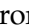







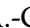

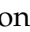
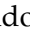

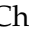



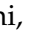
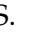


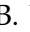





A. Attikis , K. Christoforou , S. Konstantinou , J. Mousa , C. Nicolaou, F. Ptochos , P.A. Razis , H. Rykaczewski, H. Saka , A. Stepennov 

**Charles University, Prague, Czech Republic**

M. Finger , M. Finger Jr. , A. Kveton 

**Escuela Politecnica Nacional, Quito, Ecuador**

E. Ayala 

**Universidad San Francisco de Quito, Quito, Ecuador**E. Carrera Jarrin **Academy of Scientific Research and Technology of the Arab Republic of Egypt, Egyptian Network of High Energy Physics, Cairo, Egypt**Y. Assran<sup>17,18</sup>, S. Elgammal<sup>18</sup>**Center for High Energy Physics (CHEP-FU), Fayoum University, El-Fayoum, Egypt**A. Lotfy , M.A. Mahmoud **National Institute of Chemical Physics and Biophysics, Tallinn, Estonia**R.K. Dewanjee<sup>19</sup> , K. Ehataht , M. Kadastik, T. Lange , S. Nandan , C. Nielsen , J. Pata , M. Raidal , L. Tani , C. Veelken **Department of Physics, University of Helsinki, Helsinki, Finland**H. Kirschenmann , K. Osterberg , M. Voutilainen **Helsinki Institute of Physics, Helsinki, Finland**S. Bharthuar , E. Brücken , F. Garcia , J. Havukainen , K.T.S. Kallonen , M.S. Kim , R. Kinnunen, T. Lampén , K. Lassila-Perini , S. Lehti , T. Lindén , M. Lotti, L. Martikainen , M. Myllymäki , M.m. Rantanen , H. Siikonen , E. Tuominen , J. Tuominiemi **Lappeenranta-Lahti University of Technology, Lappeenranta, Finland**P. Luukka , H. Petrow , T. Tuuva<sup>†</sup>**IRFU, CEA, Université Paris-Saclay, Gif-sur-Yvette, France**M. Besancon , F. Couderc , M. Dejardin , D. Denegri, J.L. Faure, F. Ferri , S. Ganjour , P. Gras , G. Hamel de Monchenault , V. Lohezic , J. Malcles , J. Rander, A. Rosowsky , M.Ö. Sahin , A. Savoy-Navarro<sup>20</sup> , P. Simkina , M. Titov , M. Tornago **Laboratoire Leprince-Ringuet, CNRS/IN2P3, Ecole Polytechnique, Institut Polytechnique de Paris, Palaiseau, France**C. Baldenegro Barrera , F. Beaudette , A. Buchot Perraguin , P. Busson , A. Cappati , C. Charlot , F. Damas , O. Davignon , A. De Wit , G. Falmagne , B.A. Fontana Santos Alves , S. Ghosh , A. Gilbert , R. Granier de Cassagnac , A. Hakimi , B. Harikrishnan , L. Kalipoliti , G. Liu , J. Motta , M. Nguyen , C. Ochando , L. Portales , R. Salerno , U. Sarkar , J.B. Sauvan , Y. Sirois , A. Tarabini , E. Vernazza , A. Zabi , A. Zghiche **Université de Strasbourg, CNRS, IPHC UMR 7178, Strasbourg, France**J.-L. Agram<sup>21</sup> , J. Andrea , D. Apparou , D. Bloch , J.-M. Brom , E.C. Chabert , C. Collard , S. Falke , U. Goerlach , C. Grimault, R. Haeberle , A.-C. Le Bihan , M.A. Sessini , P. Van Hove **Institut de Physique des 2 Infinis de Lyon (IP2I), Villeurbanne, France**S. Beauceron , B. Blancon , G. Boudoul , N. Chanon , J. Choi , D. Contardo , P. Depasse , C. Dozen<sup>22</sup> , H. El Mamouni, J. Fay , S. Gascon , M. Gouzevitch , C. Greenberg, G. Grenier , B. Ille , I.B. Laktineh, M. Lethuillier , L. Mirabito, S. Perries, A. Purohit , M. Vander Donckt , P. Verdier , J. Xiao **Georgian Technical University, Tbilisi, Georgia**G. Adamov, I. Lomidze , Z. Tsamalaidze<sup>16</sup> **RWTH Aachen University, I. Physikalisches Institut, Aachen, Germany**





**Greece**

G. Anagnostou, P. Assiouras , G. Daskalakis , A. Kyriakis, A. Papadopoulos<sup>31</sup>, A. Stakia 







**National and Kapodistrian University of Athens, Athens, Greece**

P. Kontaxakis , G. Melachroinos, A. Panagiotou, I. Papavergou , I. Paraskevas , N. Saoulidou , K. Theofilatos , E. Tziaferi , K. Vellidis , I. Zisopoulos 

**National Technical University of Athens, Athens, Greece**

G. Bakas , T. Chatzistavrou, G. Karapostoli , K. Kousouris , I. Papakrivopoulos , E. Siamarkou, G. Tsipolitis, A. Zacharopoulou






**University of Ioánnina, Ioánnina, Greece**

K. Adamidis, I. Bestintzanos, I. Evangelou , C. Foudas, P. Gianneios , C. Kamtsikis, P. Katsoulis, P. Kokkas , P.G. Kosmoglou Kioseoglou , N. Manthos , I. Papadopoulos , J. Strologas 



**MTA-ELTE Lendület CMS Particle and Nuclear Physics Group, Eötvös Loránd University, Budapest, Hungary**

M. Csanád , K. Farkas , M.M.A. Gadallah<sup>32</sup> , Á. Kadlecik , P. Major , K. Mandal , G. Pásztor , A.J. Rádl<sup>33</sup> , G.I. Veres 

**Wigner Research Centre for Physics, Budapest, Hungary**

M. Bartók<sup>34</sup> , C. Hajdu , D. Horvath<sup>35,36</sup> , F. Sikler , V. Veszpremi 




**Faculty of Informatics, University of Debrecen, Debrecen, Hungary**

P. Raics, B. Ujvari<sup>37</sup> , G. Zilizi 







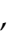
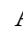







**Institute of Nuclear Research ATOMKI, Debrecen, Hungary**

G. Bencze, S. Czellar, J. Karancsi<sup>34</sup> , J. Molnar, Z. Szillasi

**Karoly Robert Campus, MATE Institute of Technology, Gyongyos, Hungary**

T. Csorgo<sup>33</sup> , F. Nemes<sup>33</sup> , T. Novak 

**Panjab University, Chandigarh, India**

J. Babbar , S. Bansal , S.B. Beri, V. Bhatnagar , G. Chaudhary , S. Chauhan , N. Dhingra<sup>38</sup> , R. Gupta, A. Kaur , A. Kaur , H. Kaur , M. Kaur , S. Kumar , M. Meena , K. Sandeep , T. Sheokand, J.B. Singh , A. Singla 













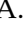


**University of Delhi, Delhi, India**

A. Ahmed , A. Bhardwaj , A. Chhetri , B.C. Choudhary , A. Kumar , M. Naimuddin , K. Ranjan , S. Saumya 

**Saha Institute of Nuclear Physics, HBNI, Kolkata, India**

S. Acharya<sup>39</sup>, S. Baradia , S. Barman<sup>40</sup> , S. Bhattacharya , D. Bhowmik, S. Dutta , S. Dutta, B. Gomber<sup>39</sup> , P. Palit , G. Saha , B. Sahu<sup>39</sup> , S. Sarkar






**Indian Institute of Technology Madras, Madras, India**

M.M. Ameen , P.K. Behera , S.C. Behera , S. Chatterjee , P. Jana , P. Kalbhor , J.R. Komaragiri<sup>41</sup> , D. Kumar<sup>41</sup> , L. Panwar<sup>41</sup> , R. Pradhan , P.R. Pujahari , N.R. Saha , A. Sharma , A.K. Sikdar , S. Verma 

**Tata Institute of Fundamental Research-A, Mumbai, India**

T. Aziz, I. Das , S. Dugad, M. Kumar , G.B. Mohanty , P. Suryadevara







**Tata Institute of Fundamental Research-B, Mumbai, India**

A. Bala , S. Banerjee , R.M. Chatterjee, M. Guchait , Sh. Jain , S. Karmakar 















**INFN Sezione di Trieste<sup>a</sup>, Università di Trieste<sup>b</sup>, Trieste, Italy**

S. Belforte<sup>a</sup> , V. Candelise<sup>a,b</sup> , M. Casarsa<sup>a</sup> , F. Cossutti<sup>a</sup> , K. De Leo<sup>a,b</sup> ,  
G. Della Ricca<sup>a,b</sup> 





**Kyungpook National University, Daegu, Korea**

S. Dogra , J. Hong , C. Huh , B. Kim , D.H. Kim , J. Kim, H. Lee, S.W. Lee ,  
C.S. Moon , Y.D. Oh , M.S. Ryu , S. Sekmen , Y.C. Yang 


**Chonnam National University, Institute for Universe and Elementary Particles, Kwangju, Korea**

G. Bak , P. Gwak , H. Kim , D.H. Moon 

**Hanyang University, Seoul, Korea**

E. Asilar , D. Kim , T.J. Kim , J.A. Merlin, J. Park 

**Korea University, Seoul, Korea**

S. Choi , S. Han, B. Hong , K. Lee, K.S. Lee , S. Lee , J. Park, S.K. Park, J. Yoo 

**Kyung Hee University, Department of Physics, Seoul, Korea**

J. Goh 









**Sejong University, Seoul, Korea**

H. S. Kim , Y. Kim, S. Lee



**Seoul National University, Seoul, Korea**

J. Almond, J.H. Bhyun, J. Choi , W. Jun , J. Kim , J.S. Kim, S. Ko , H. Kwon , H. Lee ,  
J. Lee , J. Lee , B.H. Oh , S.B. Oh , H. Seo , U.K. Yang, I. Yoon 

**University of Seoul, Seoul, Korea**

W. Jang , D.Y. Kang, Y. Kang , S. Kim , B. Ko, J.S.H. Lee , Y. Lee , I.C. Park , Y. Roh,  
I.J. Watson , S. Yang 


**Yonsei University, Department of Physics, Seoul, Korea**

S. Ha , H.D. Yoo 

**Sungkyunkwan University, Suwon, Korea**

M. Choi , M.R. Kim , H. Lee, Y. Lee , I. Yu 


**College of Engineering and Technology, American University of the Middle East (AUM), Dasman, Kuwait**

T. Beyrouthy, Y. Maghrbi 

**Riga Technical University, Riga, Latvia**

K. Dreimanis , A. Gaile , G. Pikurs, A. Potrebko , M. Seidel , V. Veckalns<sup>56</sup> 

**University of Latvia (LU), Riga, Latvia**

N.R. Strautnieks 







**Vilnius University, Vilnius, Lithuania**

M. Ambrozas , A. Juodagalvis , A. Rinkevicius , G. Tamulaitis 






**National Centre for Particle Physics, Universiti Malaya, Kuala Lumpur, Malaysia**

N. Bin Norjoharuddeen , I. Yusuff<sup>57</sup> , Z. Zolkapli

**Universidad de Sonora (UNISON), Hermosillo, Mexico**

J.F. Benitez , A. Castaneda Hernandez , H.A. Encinas Acosta, L.G. Gallegos Maríñez,  
M. León Coello , J.A. Murillo Quijada , A. Sehrawat , L. Valencia Palomo 

**Centro de Investigacion y de Estudios Avanzados del IPN, Mexico City, Mexico**

G. Ayala , H. Castilla-Valdez , E. De La Cruz-Burelo , I. Heredia-De La Cruz<sup>58</sup> ,  
R. Lopez-Fernandez , C.A. Mondragon Herrera, A. Sánchez Hernández 

**Universidad Iberoamericana, Mexico City, Mexico**

C. Oropeza Barrera , M. Ramírez García 

**Benemerita Universidad Autonoma de Puebla, Puebla, Mexico**

I. Bautista , I. Pedraza , H.A. Salazar Ibarguen , C. Uribe Estrada 

**University of Montenegro, Podgorica, Montenegro**

I. Bubanja, N. Raicevic 

**University of Canterbury, Christchurch, New Zealand**

P.H. Butler 

**National Centre for Physics, Quaid-I-Azam University, Islamabad, Pakistan**

A. Ahmad , M.I. Asghar, A. Awais , M.I.M. Awan, H.R. Hoorani , W.A. Khan 







**AGH University of Krakow, Faculty of Computer Science, Electronics and Telecommunications, Krakow, Poland**

V. Avati, L. Grzanka , M. Malawski 






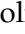








**National Centre for Nuclear Research, Swierk, Poland**

H. Bialkowska , M. Bluj , B. Boimska , M. Górski , M. Kazana , M. Szeleper ,  
P. Zalewski 



**Institute of Experimental Physics, Faculty of Physics, University of Warsaw, Warsaw, Poland**

K. Bunkowski , K. Doroba , A. Kalinowski , M. Konecki , J. Krolikowski ,  
A. Muhammad 

**Laboratório de Instrumentação e Física Experimental de Partículas, Lisboa, Portugal**

M. Araujo , D. Bastos , C. Beirão Da Cruz E Silva , A. Boletti , M. Bozzo , P. Faccioli ,  
M. Gallinaro , J. Hollar , N. Leonardo , T. Niknejad , A. Petrilli , M. Pisano ,  
J. Seixas , J. Varela , J.W. Wulff




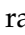
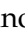






















**Faculty of Physics, University of Belgrade, Belgrade, Serbia**

P. Adzic , P. Milenovic 

**VINCA Institute of Nuclear Sciences, University of Belgrade, Belgrade, Serbia**

M. Dordevic , J. Milosevic , V. Rekovic

**Centro de Investigaciones Energéticas Medioambientales y Tecnológicas (CIEMAT), Madrid, Spain**

M. Aguilar-Benitez, J. Alcaraz Maestre , Cristina F. Bedoya , M. Cepeda , M. Cerrada , N. Colino , B. De La Cruz , A. Delgado Peris , D. Fernández Del Val ,  
J.P. Fernández Ramos , J. Flix , M.C. Fouz , O. Gonzalez Lopez , S. Goy Lopez ,  
J.M. Hernandez , M.I. Josa , J. León Holgado , D. Moran , C. M. Morcillo Perez ,  
Á. Navarro Tobar , C. Perez Dengra , A. Pérez-Calero Yzquierdo , J. Puerta Pelayo ,  
I. Redondo , D.D. Redondo Ferrero , L. Romero, S. Sánchez Navas , L. Urda Gómez ,  
J. Vazquez Escobar , C. Willmott

**Universidad Autónoma de Madrid, Madrid, Spain**

J.F. de Trocóniz 

**Universidad de Oviedo, Instituto Universitario de Ciencias y Tecnologías Espaciales de**





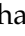







































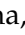
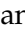
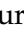




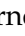
**Northwestern University, Evanston, Illinois, USA**

S. Bhattacharya , J. Bueghly, Z. Chen , K.A. Hahn , Y. Liu , Y. Miao , D.G. Monk , M.H. Schmitt , A. Taliercio , M. Velasco


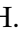

















**University of Notre Dame, Notre Dame, Indiana, USA**

R. Band , R. Bucci, S. Castells , M. Cremonesi, A. Das , R. Goldouzian , M. Hildreth , K.W. Ho , K. Hurtado Anampa , C. Jessop , K. Lannon , J. Lawrence , N. Loukas , L. Lutton , J. Mariano, N. Marinelli, I. Mcalister, T. McCauley , C. Mcgrady , C. Moore , Y. Musienko<sup>16</sup> , H. Nelson , M. Osherson , R. Ruchti , A. Townsend , M. Wayne , H. Yockey, M. Zarucki , L. Zygala 

**The Ohio State University, Columbus, Ohio, USA**

A. Basnet , B. Bylsma, M. Carrigan , L.S. Durkin , C. Hill , M. Joyce , A. Lesauvage , M. Nunez Ornelas , K. Wei, B.L. Winer , B. R. Yates 















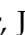

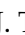

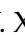

**Princeton University, Princeton, New Jersey, USA**

F.M. Addesa , H. Bouchamaoui , P. Das , G. Dezoort , P. Elmer , A. Frankenthal , B. Greenberg , N. Haubrich , S. Higginbotham , G. Kopp , S. Kwan , D. Lange , A. Loeliger , D. Marlow , I. Ojalvo , J. Olsen , A. Shevelev , D. Stickland , C. Tully 


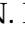

**University of Puerto Rico, Mayaguez, Puerto Rico, USA**

S. Malik 


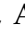





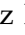
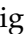




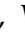
**Purdue University, West Lafayette, Indiana, USA**

A.S. Bakshi , V.E. Barnes , S. Chandra , R. Chawla , S. Das , A. Gu , L. Gutay, M. Jones , A.W. Jung , D. Kondratyev , A.M. Koshy, M. Liu , G. Negro , N. Neumeister , G. Paspalaki , S. Piperov , V. Scheurer, J.F. Schulte , M. Stojanovic , J. Thieman , A. K. Viridi , F. Wang , W. Xie 


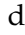









**Purdue University Northwest, Hammond, Indiana, USA**

J. Dolen , N. Parashar , A. Pathak 


**Rice University, Houston, Texas, USA**

D. Acosta , A. Baty , T. Carnahan , S. Dildick , K.M. Ecklund , P.J. Fernández Manteca , S. Freed, P. Gardner, F.J.M. Geurts , A. Kumar , W. Li , O. Miguel Colin , B.P. Padley , R. Redjimi, J. Rotter , E. Yigitbasi , Y. Zhang 

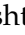















**University of Rochester, Rochester, New York, USA**

A. Bodek , P. de Barbaro , R. Demina , J.L. Dulemba , C. Fallon, A. Garcia-Bellido , O. Hindrichs , A. Khukhunaishvili , P. Parygin<sup>85</sup> , E. Popova<sup>85</sup> , R. Taus , G.P. Van Onsem 

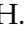






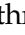
**The Rockefeller University, New York, New York, USA**

K. Goulios 















**Rutgers, The State University of New Jersey, Piscataway, New Jersey, USA**

B. Chiarito, J.P. Chou , Y. Gershtein , E. Halkiadakis , A. Hart , M. Heindl , D. Jaroslowski , O. Karacheban<sup>29</sup> , I. Laflotte , A. Lath , R. Montalvo, K. Nash, H. Routray , S. Salur , S. Schnetzer, S. Somalwar , R. Stone , S.A. Thayil , S. Thomas, J. Vora , H. Wang 






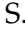





**University of Tennessee, Knoxville, Tennessee, USA**

H. Acharya, D. Ally , A.G. Delannoy , S. Fiorendi , T. Holmes , N. Karunarathna , L. Lee , E. Nibigira , S. Spanier 

**Texas A&M University, College Station, Texas, USA**

D. Aebi , M. Ahmad , O. Bouhali<sup>96</sup> , M. Dalchenko , R. Eusebi , J. Gilmore , T. Huang , T. Kamon<sup>97</sup> , H. Kim , S. Luo , S. Malhotra, R. Mueller , D. Overton , D. Rathjens , A. Safonov 









**Texas Tech University, Lubbock, Texas, USA**

N. Akchurin , J. Damgov , V. Hegde , A. Hussain , Y. Kazhykarim, K. Lamichhane , S.W. Lee , A. Mankel , T. Mengke, S. Muthumuni , T. Peltola , I. Volobouev , A. Whitbeck 

**Vanderbilt University, Nashville, Tennessee, USA**

E. Appelt , S. Greene, A. Gurrola , W. Johns , R. Kunnawalkam Elayavalli , A. Melo , F. Romeo , P. Sheldon , S. Tuo , J. Velkovska , J. Viinikainen 

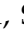



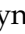
















**University of Virginia, Charlottesville, Virginia, USA**

B. Cardwell , B. Cox , J. Hakala , R. Hirosky , A. Ledovskoy , A. Li , C. Neu , C.E. Perez Lara 

**Wayne State University, Detroit, Michigan, USA**

P.E. Karchin 

**University of Wisconsin - Madison, Madison, Wisconsin, USA**

A. Aravind, S. Banerjee , K. Black , T. Bose , S. Dasu , I. De Bruyn , P. Everaerts , C. Galloni, H. He , M. Herndon , A. Herve , C.K. Koraka , A. Lanaro, R. Loveless , J. Madhusudanan Sreekala , A. Mallampalli , A. Mohammadi , S. Mondal, G. Parida , D. Pinna, A. Savin, V. Shang , V. Sharma , W.H. Smith , D. Teague, H.F. Tsoi , W. Vetens , A. Warden 

**Authors affiliated with an institute or an international laboratory covered by a cooperation agreement with CERN**

S. Afanasiev , V. Andreev , Yu. Andreev , T. Aushev , M. Azarkin , I. Azhgirey , A. Babaev , A. Belyaev , V. Blinov<sup>98</sup>, E. Boos , V. Borshch , D. Budkouski , V. Bunichev , M. Chadeeva<sup>98</sup> , V. Chekhovsky, R. Chistov<sup>98</sup> , A. Dermenev , T. Dimova<sup>98</sup> , D. Druzhkin<sup>99</sup> , M. Dubinin<sup>89</sup> , L. Dudko , A. Ershov , G. Gavrilo , V. Gavrilo , S. Gninenko , V. Golovtcov , N. Golubev , I. Golutvin , I. Gorbunov , A. Gribushin , Y. Ivanov , V. Kachanov , L. Kardapoltsev<sup>98</sup> , V. Karjavine , A. Karneyev , V. Kim<sup>98</sup> , M. Kirakosyan, D. Kirpichnikov , M. Kirsanov , V. Klyukhin , O. Kodolova<sup>100</sup> , D. Konstantinov , V. Korenkov , A. Kozyrev<sup>98</sup> , N. Krasnikov , A. Lanev , P. Levchenko<sup>101</sup> , N. Lychkovskaya , V. Makarenko , A. Malakhov , V. Matveev<sup>98</sup> , V. Murzin , A. Nikitenko<sup>102,100</sup> , S. Obraztsov , V. Oreshkin , V. Palichik , V. Perelygin , M. Perfilov, S. Polikarpov<sup>98</sup> , V. Popov, O. Radchenko<sup>98</sup> , R. Ryutin, M. Savina , V. Savrin , V. Shalaev , S. Shmatov , S. Shulha , Y. Skovpen<sup>98</sup> , S. Slabospitskii , V. Smirnov , A. Snigirev , D. Sosnov , V. Sulimov , E. Tcherniaev , A. Terkulov , O. Teryaev , I. Tlisova , A. Toropin , L. Uvarov , A. Uzunian , A. Volkov, A. Vorobyev<sup>†</sup>, N. Voytishin , B.S. Yuldashev<sup>103</sup>, A. Zarubin , I. Zhizhin , A. Zhokin 

†: Deceased

<sup>1</sup>Also at Yerevan State University, Yerevan, Armenia

<sup>2</sup>Also at TU Wien, Vienna, Austria

<sup>3</sup>Also at Institute of Basic and Applied Sciences, Faculty of Engineering, Arab Academy for Science, Technology and Maritime Transport, Alexandria, Egypt

<sup>4</sup>Also at Ghent University, Ghent, Belgium

- 
- <sup>5</sup>Also at Universidade Estadual de Campinas, Campinas, Brazil
- <sup>6</sup>Also at Federal University of Rio Grande do Sul, Porto Alegre, Brazil
- <sup>7</sup>Also at UFMS, Nova Andradina, Brazil
- <sup>8</sup>Also at Nanjing Normal University, Nanjing, China
- <sup>9</sup>Now at Henan Normal University, Xinxiang, China
- <sup>10</sup>Now at The University of Iowa, Iowa City, Iowa, USA
- <sup>11</sup>Also at University of Chinese Academy of Sciences, Beijing, China
- <sup>12</sup>Also at China Center of Advanced Science and Technology, Beijing, China
- <sup>13</sup>Also at University of Chinese Academy of Sciences, Beijing, China
- <sup>14</sup>Also at China Spallation Neutron Source, Guangdong, China
- <sup>15</sup>Also at Université Libre de Bruxelles, Bruxelles, Belgium
- <sup>16</sup>Also at an institute or an international laboratory covered by a cooperation agreement with CERN
- <sup>17</sup>Also at Suez University, Suez, Egypt
- <sup>18</sup>Now at British University in Egypt, Cairo, Egypt
- <sup>19</sup>Also at Birla Institute of Technology, Mesra, Mesra, India
- <sup>20</sup>Also at Purdue University, West Lafayette, Indiana, USA
- <sup>21</sup>Also at Université de Haute Alsace, Mulhouse, France
- <sup>22</sup>Also at Department of Physics, Tsinghua University, Beijing, China
- <sup>23</sup>Also at The University of the State of Amazonas, Manaus, Brazil
- <sup>24</sup>Also at Erzincan Binali Yildirim University, Erzincan, Turkey
- <sup>25</sup>Also at University of Hamburg, Hamburg, Germany
- <sup>26</sup>Also at RWTH Aachen University, III. Physikalisches Institut A, Aachen, Germany
- <sup>27</sup>Also at Isfahan University of Technology, Isfahan, Iran
- <sup>28</sup>Also at Bergische University Wuppertal (BUW), Wuppertal, Germany
- <sup>29</sup>Also at Brandenburg University of Technology, Cottbus, Germany
- <sup>30</sup>Also at Forschungszentrum Jülich, Juelich, Germany
- <sup>31</sup>Also at CERN, European Organization for Nuclear Research, Geneva, Switzerland
- <sup>32</sup>Also at Physics Department, Faculty of Science, Assiut University, Assiut, Egypt
- <sup>33</sup>Also at Wigner Research Centre for Physics, Budapest, Hungary
- <sup>34</sup>Also at Institute of Physics, University of Debrecen, Debrecen, Hungary
- <sup>35</sup>Also at Institute of Nuclear Research ATOMKI, Debrecen, Hungary
- <sup>36</sup>Now at Universitatea Babeş-Bolyai - Facultatea de Fizica, Cluj-Napoca, Romania
- <sup>37</sup>Also at Faculty of Informatics, University of Debrecen, Debrecen, Hungary
- <sup>38</sup>Also at Punjab Agricultural University, Ludhiana, India
- <sup>39</sup>Also at University of Hyderabad, Hyderabad, India
- <sup>40</sup>Also at University of Visva-Bharati, Santiniketan, India
- <sup>41</sup>Also at Indian Institute of Science (IISc), Bangalore, India
- <sup>42</sup>Also at IIT Bhubaneswar, Bhubaneswar, India
- <sup>43</sup>Also at Institute of Physics, Bhubaneswar, India
- <sup>44</sup>Also at Department of Physics, Isfahan University of Technology, Isfahan, Iran
- <sup>45</sup>Also at Sharif University of Technology, Tehran, Iran
- <sup>46</sup>Also at Department of Physics, University of Science and Technology of Mazandaran, Behshahr, Iran
- <sup>47</sup>Also at Helwan University, Cairo, Egypt
- <sup>48</sup>Also at Italian National Agency for New Technologies, Energy and Sustainable Economic Development, Bologna, Italy
- <sup>49</sup>Also at Centro Siciliano di Fisica Nucleare e di Struttura Della Materia, Catania, Italy
- <sup>50</sup>Also at Università degli Studi Guglielmo Marconi, Roma, Italy

- <sup>51</sup>Also at Scuola Superiore Meridionale, Università di Napoli 'Federico II', Napoli, Italy
- <sup>52</sup>Also at Fermi National Accelerator Laboratory, Batavia, Illinois, USA
- <sup>53</sup>Also at Università di Napoli 'Federico II', Napoli, Italy
- <sup>54</sup>Also at Ain Shams University, Cairo, Egypt
- <sup>55</sup>Also at Consiglio Nazionale delle Ricerche - Istituto Officina dei Materiali, Perugia, Italy
- <sup>56</sup>Also at Riga Technical University, Riga, Latvia
- <sup>57</sup>Also at Department of Applied Physics, Faculty of Science and Technology, Universiti Kebangsaan Malaysia, Bangi, Malaysia
- <sup>58</sup>Also at Consejo Nacional de Ciencia y Tecnología, Mexico City, Mexico
- <sup>59</sup>Also at Trincomalee Campus, Eastern University, Sri Lanka, Nilaveli, Sri Lanka
- <sup>60</sup>Also at Saegis Campus, Nugegoda, Sri Lanka
- <sup>61</sup>Also at INFN Sezione di Pavia, Università di Pavia, Pavia, Italy
- <sup>62</sup>Also at National and Kapodistrian University of Athens, Athens, Greece
- <sup>63</sup>Also at Ecole Polytechnique Fédérale Lausanne, Lausanne, Switzerland
- <sup>64</sup>Also at University of Vienna Faculty of Computer Science, Vienna, Austria
- <sup>65</sup>Also at Universität Zürich, Zurich, Switzerland
- <sup>66</sup>Also at Stefan Meyer Institute for Subatomic Physics, Vienna, Austria
- <sup>67</sup>Also at Laboratoire d'Annecy-le-Vieux de Physique des Particules, IN2P3-CNRS, Annecy-le-Vieux, France
- <sup>68</sup>Also at Near East University, Research Center of Experimental Health Science, Mersin, Turkey
- <sup>69</sup>Also at Konya Technical University, Konya, Turkey
- <sup>70</sup>Also at Izmir Bakircay University, Izmir, Turkey
- <sup>71</sup>Also at Adiyaman University, Adiyaman, Turkey
- <sup>72</sup>Also at Bozok Universitetesi Rektörlüğü, Yozgat, Turkey
- <sup>73</sup>Also at Marmara University, Istanbul, Turkey
- <sup>74</sup>Also at Milli Savunma University, Istanbul, Turkey
- <sup>75</sup>Also at Kafkas University, Kars, Turkey
- <sup>76</sup>Now at Istanbul Okan University, Istanbul, Turkey
- <sup>77</sup>Also at Hacettepe University, Ankara, Turkey
- <sup>78</sup>Also at Istanbul University - Cerrahpasa, Faculty of Engineering, Istanbul, Turkey
- <sup>79</sup>Also at Yildiz Technical University, Istanbul, Turkey
- <sup>80</sup>Also at Vrije Universiteit Brussel, Brussel, Belgium
- <sup>81</sup>Also at School of Physics and Astronomy, University of Southampton, Southampton, United Kingdom
- <sup>82</sup>Also at University of Bristol, Bristol, United Kingdom
- <sup>83</sup>Also at IPPP Durham University, Durham, United Kingdom
- <sup>84</sup>Also at Monash University, Faculty of Science, Clayton, Australia
- <sup>85</sup>Now at an institute or an international laboratory covered by a cooperation agreement with CERN
- <sup>86</sup>Also at Università di Torino, Torino, Italy
- <sup>87</sup>Also at Bethel University, St. Paul, Minnesota, USA
- <sup>88</sup>Also at Karamanoğlu Mehmetbey University, Karaman, Turkey
- <sup>89</sup>Also at California Institute of Technology, Pasadena, California, USA
- <sup>90</sup>Also at United States Naval Academy, Annapolis, Maryland, USA
- <sup>91</sup>Also at Bingol University, Bingol, Turkey
- <sup>92</sup>Also at Georgian Technical University, Tbilisi, Georgia
- <sup>93</sup>Also at Sinop University, Sinop, Turkey
- <sup>94</sup>Also at Erciyes University, Kayseri, Turkey

<sup>95</sup>Also at Horia Hulubei National Institute of Physics and Nuclear Engineering (IFIN-HH), Bucharest, Romania

<sup>96</sup>Also at Texas A&M University at Qatar, Doha, Qatar

<sup>97</sup>Also at Kyungpook National University, Daegu, Korea

<sup>98</sup>Also at another institute or international laboratory covered by a cooperation agreement with CERN

<sup>99</sup>Also at Universiteit Antwerpen, Antwerpen, Belgium

<sup>100</sup>Also at Yerevan Physics Institute, Yerevan, Armenia

<sup>101</sup>Also at Northeastern University, Boston, Massachusetts, USA

<sup>102</sup>Also at Imperial College, London, United Kingdom

<sup>103</sup>Also at Institute of Nuclear Physics of the Uzbekistan Academy of Sciences, Tashkent, Uzbekistan